

# Long-term motor cortical map changes following unilateral lesion of the hand representation in the motor cortex in macaque monkeys showing functional recovery of hand functions

Alexander F. Wyss<sup>a,1</sup>, Adjia Hamadjida<sup>a,d,1</sup>, Julie Savidan<sup>a,1</sup>, Yu Liu<sup>a,e</sup>, Shahid Bashir<sup>a,f</sup>, Anis Mir<sup>b</sup>, Martin E. Schwab<sup>c</sup>, Eric M. Rouiller<sup>a,\*</sup> and Abderaouf Belhaj-Saif<sup>a,2</sup>

<sup>a</sup>*Faculty of Sciences and Fribourg Centre for Cognition, Department of Medicine, University of Fribourg, Chemin du Musée, Fribourg, Switzerland*

<sup>b</sup>*Novartis Pharma AG, Basel, Switzerland*

<sup>c</sup>*Brain Research Institute, University of Zürich and Department of Health Sciences and Technology, ETH Zürich, Switzerland*

<sup>d</sup>*Université de Montréal, Département de Physiologie, Chemin de la Tour, Montréal QC, Canada*

<sup>e</sup>*Univ. Tennessee HSC, Memphis, TN, USA*

<sup>f</sup>*Faculty of Medicine, Department of Physiology, Autism Research and Treatment Center, King Saud University, Riyadh, Saudi Arabia and Berenson-Allen Center for Noninvasive Brain Stimulation, Department of Neurology, Beth Israel Deaconess Medical Center, Harvard Medical School, Boston, MA, USA*

## Abstract.

**Purpose:** How are motor maps modified within and in the immediate vicinity of a damaged zone in the motor cortex of non-human primates?

**Methods:** In eight adult macaque monkeys subjected to a restricted chemical lesion of the hand area in the primary motor cortex (M1), motor maps were established using intracortical micro-stimulation (ICMS) techniques. The monkeys were subdivided into five animals without treatment, whereas three monkeys received an anti-Nogo-A antibody treatment.

**Results:** Following permanent M1 injury, the lesion territory became largely non micro-excitabile several months post-lesion, in spite of some recovery of hand function. Few sites within the lesion territory remained excitable, though irrespective to the degree of functional recovery. Around the lesion in M1, there was no reallocation of proximal shoulder/arm territories into distal hand functions. However, ICMS delivered at supra-threshold intensities in these proximal territories elicited digit movements. Post-lesion ICMS thresholds to elicit movements of forelimb muscle territories increased, independently from the degree of functional recovery. Further behavioural evidence for an enhancement of functional recovery promoted by the anti-Nogo-A antibody treatment is provided.

**Conclusion:** The degree of functional recovery is not related to a reorganization of motor maps within, and in the vicinity of, a M1 lesion.

**Keywords:** Primates, intracortical microstimulation, somatotopy, neuroplasticity

<sup>1</sup>Equal first authorship.

<sup>2</sup>Equal senior authorship.

\*Corresponding author: Prof. Eric M. Rouiller, Department of Medicine, University of Fribourg, Chemin du Musée 5, CH-1700 Fribourg, Switzerland. Tel.: +41 26 300 86 09; Fax: +41 26 300 96 75; E-mail: Eric.Rouiller@unifr.ch.

## 1. Introduction

A lesion of the adult motor cortex results in a long-lasting hemi-paresis of the corresponding (opposite) body territory, although some spontaneous and incomplete functional recovery may occur during the weeks or months following the cortical damage (see e.g. Dancause and Nudo, 2011 for review). Knowledge of the mechanisms underlying this limited spontaneous recovery is crucial in order to develop strategies to enhance functional restitution from cortical damage, using rehabilitative training protocols and/or various treatments (pharmacological, cell therapy, brain stimulation, etc). Before clinical application can be done safely and efficiently, mechanisms of functional restitution should be elucidated in detail using animal models. In this context, the model of the non-human primate is especially valuable as the general organization of the motor system controlling voluntary movements in monkeys is similar to that of humans (Courtine et al., 2007; Lemon and Griffiths 2005; Lemon, 2008). In the past, several studies conducted in non-human primates have investigated the consequences (deficits) of a lesion of the motor cortex on the ability to perform voluntary movements, as well as to what extent and how some spontaneous recovery may contribute to the restitution of some motor control (e.g. Ogden and Franz, 1917; Glees and Cole, 1950; Travis, 1955; Brinkman and Kuypers, 1973; Passingham et al., 1983; Friel and Nudo, 1998; Rouiller, et al., 1998; Liu and Rouiller, 1999; Frost et al., 2003; Marshall et al., 2003; Plautz et al., 2003; Roitberg et al., 2003; Dancause et al., 2005, 2006; Pizzimenti et al., 2007; Eisner-Janowicz et al., 2008; Murata et al., 2008; Darling et al., 2009, 2010, 2011; Bihel et al., 2010; McNeal et al., 2010; Kaeser et al., 2010, 2011; Bashir et al., 2012; Hamadjida et al., 2012). The usually incomplete spontaneous recovery taking place after a unilateral lesion affecting the primary motor cortex (M1) is based, at least in part, on a vicarious phenomenon in which (ipsilesional) non-primary motor cortical areas (premotor cortex (PM), Supplementary motor area (SMA), or even the somatosensory cortex) may take over part of the lost function (Sasaki and Gemba, 1984; Widener and Cheney, 1997; Liu and Rouiller, 1999; Frost et al., 2003; Dancause et al., 2005, 2006; Eisner-Janowicz et al., 2008; McNeal et al., 2010). The incomplete functional recovery of manual dexterity in cases where the lesion of M1 affects the hand representation may include the emergence of

compensatory movement patterns, favored by rehabilitative training (e.g. Friel and Nudo, 1998; Murata et al., 2008), or in combination with peri-infarct electrical stimulation (Plautz et al., 2003).

One may hypothesize that the more extensive (or severe) the lesion in M1, the more likely is the involvement of a non-primary motor cortical area in the incomplete functional recovery. If the lesion is however restricted to a part of M1, there is evidence that preserved territories in M1 may be re-organized to take over part of the lost motor function, if post-lesion training/practice takes place or in case of neonatal lesion (Glees and Cole, 1950; Nudo and Milliken, 1996; Nudo et al., 1996; Rouiller et al., 1998; Plautz et al., 2003). The re-organization of such peri-lesion territory in M1 consists in changes of somatotopic representations, as assessed by intracortical microstimulation (ICMS) by comparing pre-lesion and post-lesion motor maps. The goal of the present study was to investigate, in a relatively large group of eight adult macaque monkeys subjected to a restricted chemical (excitotoxic) lesion of the hand M1 representation, how the motor maps are modified within as well as at the vicinity of the damaged zone using ICMS performed pre-lesion and repeated post-lesion, after the incomplete functional recovery has reached a plateau. In other words, it is hypothesized that, as a result of ibotenic acid infusion in the hand area in M1, the lesioned territory remains non-responsive to ICMS post-lesion, in spite of an incomplete functional recovery. A further hypothesis is that the extent of functional recovery is related to the degree of motor map rearrangement in the cortical territories immediately adjacent to the lesion. Finally, the pool of eight monkeys subjected to a unilateral lesion of the motor cortex was subdivided into a subgroup of five (control) animals without treatment to improve functional recovery, and a subgroup of three monkeys which received an anti-Nogo-A antibody treatment (see Gonzenbach and Schwab, 2008; Schwab, 2010 for review on this therapy), known to enhance functional recovery after motor cortex lesion in the rat (Papadopoulos et al., 2002; Emerick et al., 2003; Emerick and Kartje, 2004; Seymour et al., 2005; Markus et al., 2005; Tsai et al., 2007, 2011; Cheatwood et al., 2008; Gillani et al., 2010). An assessment of the possible benefit of the anti-Nogo-A antibody treatment on functional recovery was conducted here from the eight monkeys, in parallel to the analysis of the electrophysiological data.

## 2. Methods

### 2.1. General survey of the experiments

The data were collected from 8 monkeys (*macaca fascicularis*, 3.5–6.5 kg, 4–6 years old, 1 female and 7 male), all trained to perform 3 different behavioral tasks aimed at assessing manual hand dexterity (Schmidlin et al., 2011; Kaeser et al., 2011, 2013; Hamadjida et al., 2012): (i) the modified Brinkman board task; (ii) the rotative Brinkman board task; (iii) the Brinkman box task (see Schmidlin et al., 2011 for a detailed description and for visualization of the 3 manual dexterity tasks). Once the monkeys attained a stable behavioral performance for several weeks (thus reaching a pre-lesion plateau), a chronic stainless steel chamber was implanted above the left hemisphere, to have access principally to the primary motor cortex (M1) and the dorsal and ventral premotor cortical areas (PMd and PMv, respectively). The hand area of M1 was defined based on a first series (pre-lesion) of daily ICMS sessions for a period of about 2 months, during which the behavioral training was pursued, though to a lesser extent. After completion of the pre-lesion ICMS map, behavioral training was more extensively repeated in order to confirm the pre-lesion plateau of manual dexterity obtained before the ICMS phase. Targeting the ICMS sites where a movement of the hand was elicited at low threshold, ibotenic acid was infused at multiple sites (Table 1) to generate a permanent lesion aimed unilaterally at the hand representation, as previously reported (Liu and Rouiller, 1999; Kaeser et al., 2010, 2011; Bashir et al., 2012; Hamadjida et al., 2012). The behavioral assessment was conducted daily over several months to quantify the deficits resulting from the lesion as well as the time course and extent of functional recovery during several months post-lesion (see Kaeser et al., 2010, 2011; Bashir et al., 2012; Hamadjida et al., 2012). After reaching a post-lesion plateau of behavioral recovery, stable over a few weeks, a second (post-lesion) series of daily ICMS session was performed, with the aim to investigate how the initial hand representation was modified by both the lesion and the functional recovery of manual dexterity. The second series of daily ICMS sessions also lasted approximately 2 months, as the same sites were re-explored. The aim of the present study was to specifically compare the pre-lesion and the post-lesion ICMS maps.

Surgical procedures and animal care, previously described in detail (Kaeser et al., 2010, 2011; Bashir et al., 2012; Hamadjida et al., 2012), were conducted in accordance to the Guide for the Care and Use of Laboratory Animals (ISBN 0-309-05377-3; 1996). The experimental protocol was approved first by the local (cantonal) ethical committee (surveying animal experimentation and evaluating research proposals). Finally, the experiments were authorized by the cantonal (Fribourg) and federal (Swiss) veterinary officers. The present experiments were covered by the following authorizations: FR 24/95/1; FR 44/92/3; FR 157/01, FR 157/03, FR 157/04, FR 156/04, FR 156/06, FR 157e/06; FR 185-08.

### 2.2. Manual dexterity tests (behavioral assessment)

The eight monkeys were trained to perform behavioral tasks aimed at quantifying manual dexterity (see above). In the present report, behavioral data derived from the modified Brinkman board task are reported. The task, modified from the original test (Brinkman and Kyupers, 1973; Brinkman, 1984), was designed to specifically assess manual dexterity in monkeys (see Schmidlin et al., 2011 for detail). The monkey, sat in a primate chair, is placed in front of a board comprising of 50 slots, 25 oriented vertically and 25 horizontally, each filled with a food pellet. Using either the left hand or the right hand, the monkey grasped pellets using the precision grip, by opposing the tip of the index finger to the tip of the thumb. The methods of analysis of the behavioral data have been presented in a recent report (Schmidlin et al., 2011). In the present study, motor performance was assessed by the score, given by the number of pellets retrieved during the first 30 seconds of the test, from either the vertical or the horizontal slots. A total score was calculated, corresponding to the sum of the scores obtained for the 2 slots orientations.

### 2.3. Surgical procedures

All surgical procedures were conducted under deep anesthesia. Before all implant surgeries, the monkeys were sedated with an intramuscular (i.m.) injection of ketamine (Ketalar®; Parke-Davis, 5 mg/kg) and atropine was injected to reduce bronchial secretion (0.05 mg/kg, i.m.). Monkeys were then deeply anesthetized with an intravenous (i.v.) perfusion of 1% propofol (Fresenius®) mixed with a 5% glucose saline

solution (1 volume propofol and 2 volumes of gluco-saline, delivered at a dose of 0.1 mg/kg/min). To prevent brain edema, Dexamethasone (Decadon<sup>®</sup>) was injected i.m. (0.05 ml/kg diluted 1 : 1 in saline). Concomitantly, a preventive pain killer (Carprofen) was administered i.m. (Rimadyl<sup>®</sup>; 50 mg/ml, 4 mg/kg). To further reduce possible activation of pain receptors during the surgery itself, ketamine was added to the i.v. perfusion solution (0.0625 mg/kg/min), as previously reported (Freund et al., 2007). The surgery was carried out under continuous monitoring of the following parameters: heart rate, respiration rate, expired CO<sub>2</sub>, arterial O<sub>2</sub> saturation and body temperature. Before surgery, all monkeys received a subcutaneous injection of the antibiotic Albipen<sup>®</sup> (Ampicillin 10%, 30 mg/kg). Immediately after surgery and offset of anesthesia, the monkey was continuously supervised by the experimenters until it was sufficiently awake and started to eat and drink. During the week following the surgery, additional doses of Carprofen were given daily (Rymadil<sup>®</sup> pills mixed with food, 4 mg/kg). Antibiotic (ampiciline as above) was administered on alternate days for the first week after surgery. All surgeries were performed in a facility under sterile conditions and approved by the cantonal veterinary office.

#### 2.4. Cortical chronic chamber implant

After reaching a stable behavioral performance (pre-lesion plateau), a square or a rectangular stainless steel chamber was stereotaxically implanted above the forelimb area of M1 on the left hemisphere (except in Mk-JU which was implanted above the right hemisphere). The chamber was centered at stereotaxic coordinates 15 mm anterior and 15 mm lateral, and at an angle of 30° with respect to the mid-sagittal plane, allowing perpendicular electrode penetrations with respect to the cortical surface. Six to ten self-taped titanium screws were used to anchor the chamber to the skull. Moreover, for better stability, two flat wings soldered to the chamber, one rostral and one caudal, were also anchored to the skull by titanium screws. The edge of the chronic chamber next to the skull, as well as the titanium screws were covered with dental acrylic or orthopedic cement (Palacos<sup>®</sup>). Over the mid-occipital and frontal regions of the skull, two stainless steel cylinders were anchored with 3-4 titanium screws and then cemented as described above for the chronic chamber. These cylinders allowed head restraining during the cleaning of the chronic chamber

and, most importantly, during the ICMS sessions conducted while the monkey was awake. Nevertheless, a partly flexible head restraint attached to the cylinders allowed limited movement of the head. To prevent infection, the chronic chamber was cleaned daily with Betadine and an antibiotic ointment (Morrhulan).

#### 2.5. Intracortical microstimulation (ICMS) procedures

During the initial phase of behavioral training, the monkeys were progressively habituated to be passively manipulated, allowing the experimenter to generate passive movement of the forelimb and hindlimb. The goal of this habituation was to offer the possibility to the experimenter to modify the posture of the limbs during the subsequent ICMS sessions, for better assessment (visual and by palpation) of the overt motor response elicited by the electrical ICMS and searching for the threshold. Electrophysiological ICMS procedures (see Rouiller et al., 1998; Liu and Rouiller, 1999; Schmidlin et al., 2004, 2005) were performed twice in each monkey, first before the cortical lesion in order to guide the lesion procedure by mapping the M1 hand representation and, second, several months after the lesion when the monkeys reached a stable post-lesion manual performance (Table 1).

For ICMS, we used glass- or mylar-insulated platinum-iridium electrodes with typical impedances between 0.1 to 1.0 MΩ (Frederick Haer & Co., Bowdoinham, ME). The monkey sat in the primate chair, as described previously (Liu and Rouiller, 1999). The head was restrained and the electrode advancing system (Narishige group, Japan, Model MO-95) was attached to the chronic chamber. Electrode penetrations were performed systematically in and around the hand area of M1, distributed at a 1 mm grid interval, along the rostro-caudal and medio-lateral axes (Fig. 1A). The electrode was manually advanced (usually 1 mm step in depth), starting from 2 mm below the dura surface, along a maximal distance of 10–12 mm for penetrations targeting the rostral bank of the central sulcus, as recently illustrated (Kaeser et al., 2010).

The ICMS consisted of 12 electric pulses, delivered in a train of 33 ms duration, at a rate of 330 Hz. The effect of ICMS was assessed by visual inspection and/or palpation of muscle contraction at which a movement was elicited. The minimal current (ICMS threshold) producing the motor response was determined at each ICMS site along the electrode

Table 1  
List of monkeys subjected to permanent primary motor cortex lesion and included in the present study with identification code

Gender	Mk-CE		Mk-JU		Mk-GE		Mk-RO		Mk-BI		Mk-VA		Mk-SL		Mk-MO		
	Male	None	Male	None	Female	None	Male	None	Male	None	Anti-Nogo-A antibody	Male	Anti-Nogo-A antibody	Male	Anti-Nogo-A antibody	Male	
Age at time of lesion (rounded 0.5 year)	4.5	5	5	4	5	5	4	5	5	5	5.5	5.5	5.5	5.5	5.5	5.5	5.5
Weight at time of lesion	3.8	3.6	3.6	3.2	2.8	2.8	3.2	3.2	5	5	4.9	4.9	4.6	4.6	5.6	5.6	5.6
Volume of ibotenic acid injected ( $\mu$ L)	40	40	40	18	13	13	18	29.7	29.7	29.7	15.5	15.5	18	18	20	20	20
Number of ICMS sites injected with ibotenic acid	21	21	21	12	13	13	12	29	29	29	11	11	12	12	20	20	20
Time interval (months) between lesion and post-lesion ICMS mapping	11	10	10	5	3.25	3.25	5	7.3	7.3	7.3	10.5	10.5	16.5	16.5	3.2	3.2	3.2
Estimates of "unfolded hand area pre-lesion" (in $\text{mm}^2$ )	<b>37</b>	<b>33</b>	<b>33</b>	<b>56</b>	<b>25</b>	<b>25</b>	<b>56</b>	<b>55</b>	<b>55</b>	<b>55</b>	<b>40</b>	<b>40</b>	<b>45</b>	<b>45</b>	<b>34</b>	<b>34</b>	<b>34</b>
Total volume of lesion (in $\text{mm}^3$ ) Gray matter (motor cortex + post-central gyrus)	<b>112.8</b>	<b>63.01</b>	<b>63.01</b>	<b>14</b>	<b>48.7</b>	<b>48.7</b>	<b>14</b>	<b>20.13</b>	<b>20.13</b>	<b>20.13</b>	<b>20</b>	<b>20</b>	<b>78.2</b>	<b>78.2</b>	<b>41.8</b>	<b>41.8</b>	<b>41.8</b>
Volume of lesion in post-central gyrus (in $\text{mm}^3$ )	10.1	0	0	0	7.6	7.6	0	0	0	0	5.8	5.8	1.8	1.8	0	0	0
Lesion spread sub-cortically to the white matter (in $\text{mm}^3$ )	86.5	28.9	28.9	0	0	0	0	0	0	0	0	0	130.6	130.6	0	0	0
Degree of functional recovery from M1 lesion (expressed in % of post-lesion total score at plateau with respect to pre-lesion total score in the modified Brinkman board task: all slots)	<b>42%</b>	<b>39%</b>	<b>39%</b>	<b>98%</b>	<b>38%</b>	<b>38%</b>	<b>98%</b>	<b>74%</b>	<b>74%</b>	<b>74%</b>	<b>87%</b>	<b>87%</b>	<b>73%</b>	<b>73%</b>	<b>76%</b>	<b>76%</b>	<b>76%</b>
Degree of functional recovery from M1 lesion (expressed in % of post-lesion horizontal score at plateau with respect to pre-lesion horizontal score in the modified Brinkman board task: horizontal slots)	<b>9%</b>	<b>29%</b>	<b>29%</b>	<b>90%</b>	<b>11%</b>	<b>11%</b>	<b>90%</b>	<b>36%</b>	<b>36%</b>	<b>36%</b>	<b>91%</b>	<b>91%</b>	<b>77%</b>	<b>77%</b>	<b>60%</b>	<b>60%</b>	<b>60%</b>
Degree of functional recovery from M1 lesion (expressed in % of post-lesion vertical score at plateau with respect to pre-lesion vertical score in the modified Brinkman board task: vertical slots)	<b>59%</b>	<b>46%</b>	<b>46%</b>	<b>100%</b>	<b>57%</b>	<b>57%</b>	<b>100%</b>	<b>94%</b>	<b>94%</b>	<b>94%</b>	<b>87%</b>	<b>87%</b>	<b>77%</b>	<b>77%</b>	<b>84%</b>	<b>84%</b>	<b>84%</b>

Monkeys Mk-CE and Mk-JU were part of a pilot study (Liu and Rouiller, 1999), with the initial aim to generate fairly large lesions. In subsequent monkeys (Mk-GE and Mk-VA), the volume of ibotenic acid was reduced to generate a lesion more focused to the M1 hand area. In the monkeys included later over the 8 years of the study (Mk-RO, Mk-BI, Mk-MO and Mk-SL), ibotenic acid was injected under propofol anaesthesia (as required by new ethical guidelines), and no longer in the awake state. The volume of ibotenic acid was thus slightly increased, as propofol is known to reduce the excitotoxicity of ibotenic acid (Snyder et al., 2007).

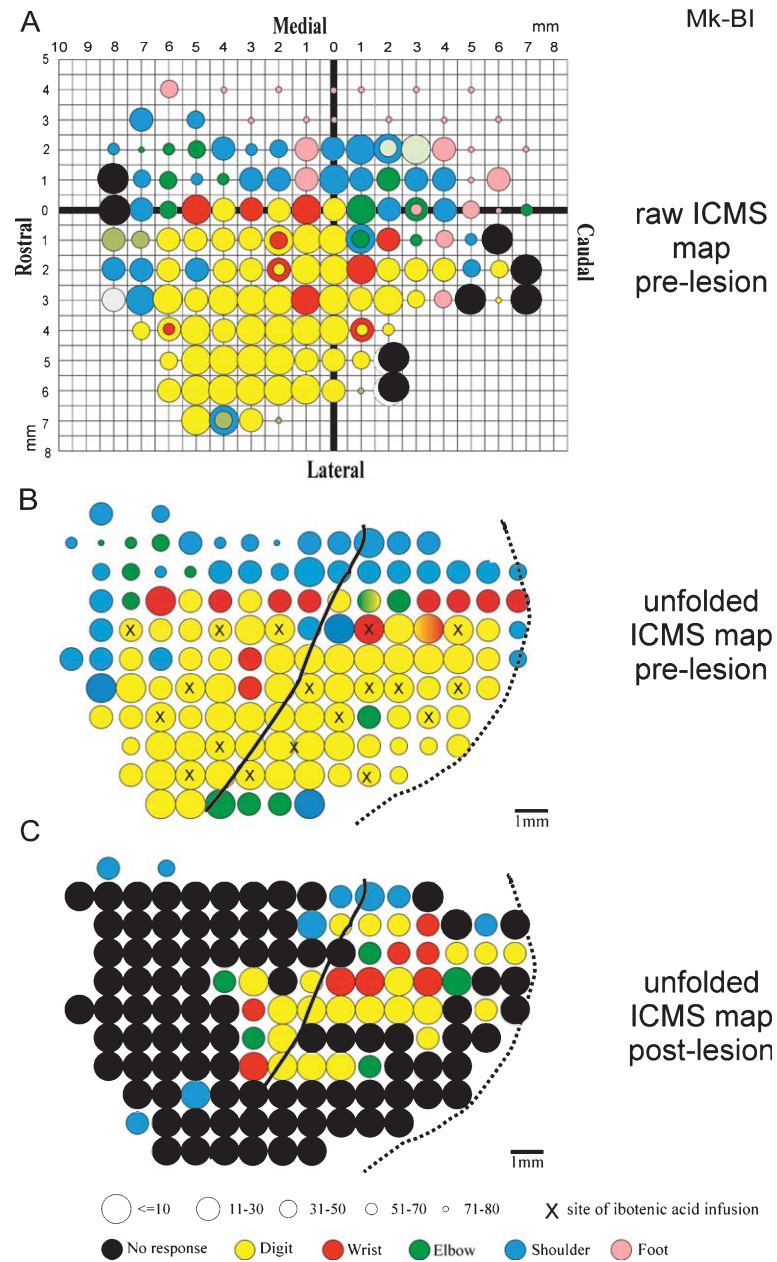


Fig. 1. Example of ICMS maps established in the untreated monkey Mk-BI, in the initial (raw) format pre-lesion (panel A) and after unfolding the central sulcus, pre-lesion (panel B) and post-lesion (panel C). In panel A, each circle corresponds to the location on the cortical surface of an electrode penetration. Still in panel A, the movement elicited by ICMS at the lowest threshold along each electrode penetration is represented by the color code shown on the bottom (e.g. wrist, finger, etc.; at few sites, a circle represented with 2 colors indicate an effect at the same threshold for two body territories). The same ICMS sites as in panel A appear in panel B and C, plus some additional sites along the rostral bank of the central sulcus, as explained in the methods. Same color code in panels B and C as in panel A. In all panels, the set of circles on the bottom of the figure indicates the threshold (in microamps) at which the corresponding body movement was still observable at the lowest intensity. The five graded circle sizes (encountered in the ICMS maps) correspond to different threshold ranges, as indicated on the right of the circles. In each ICMS map, five graded circle sizes have been used to distinguish the excitability of each ICMS site. In panels B and C, the solid oblique line represents the approximate position of the central sulcus as it appears on the surface of the cerebral cortex, whereas the oblique dashed line represents the fundus of the central sulcus.

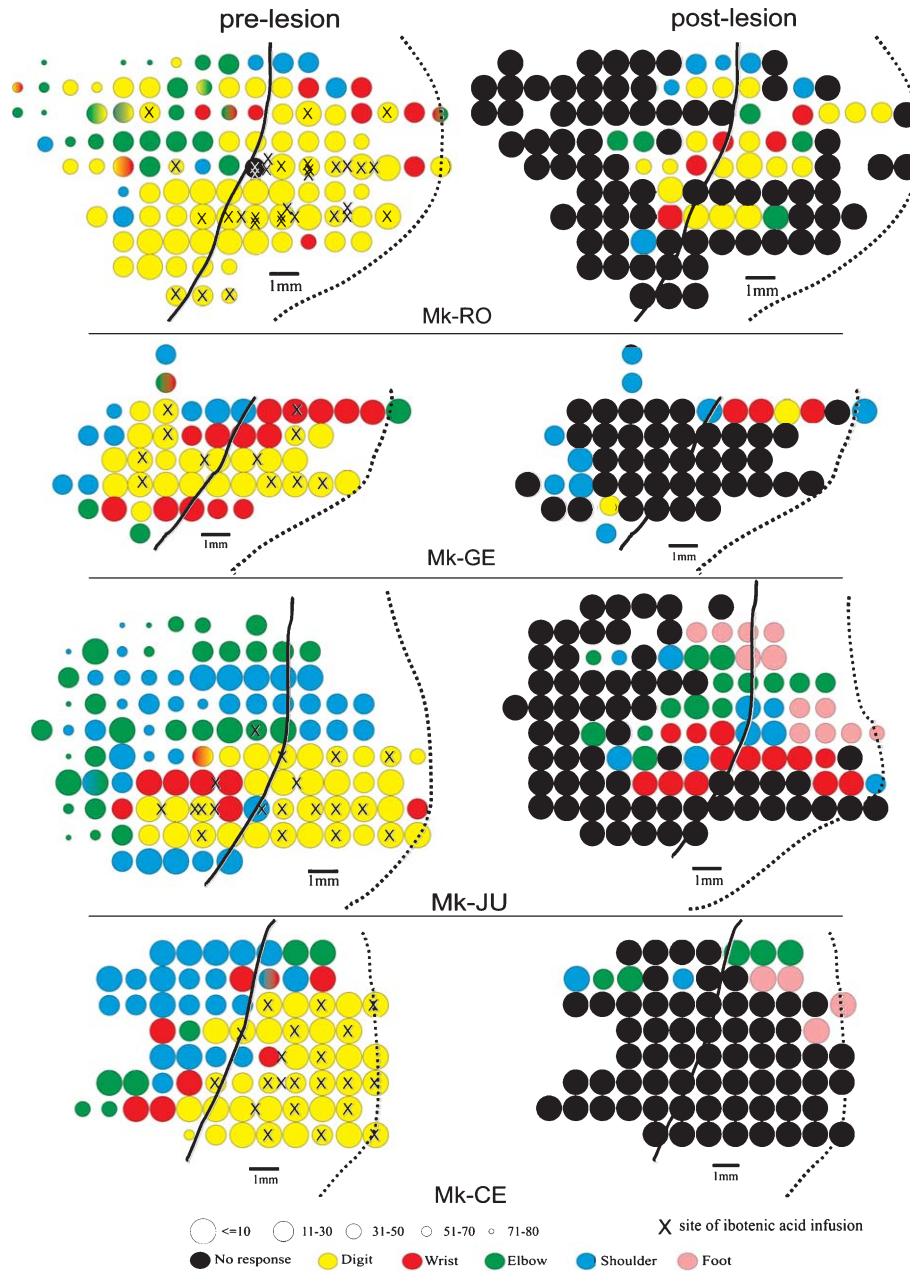


Fig. 2. Unfolded ICMS maps established pre-lesion (left column) and post-lesion (right column) in the untreated monkeys MK-RO, Mk-GE, Mk-JU and Mk-CE. same conventions as in Fig. 1. In Mk-JU, the ICMS map has been mirrored horizontally so that it appears as derived from the left hemisphere for better comparison with the other monkeys, although the mapping was conducted originally on the right hemisphere (see Fig. 4A: Mk-JU).

penetration. The intensity of stimulation ranged from 80 to 1 microamp. The intensity of 80 microamps was mostly applied at the beginning of the electrode penetration (close to surface) and was decreased until

threshold. At the next ICMS site (1 mm deeper), the initial intensity of stimulation was set slightly above (10 microamps) the threshold intensity of the previous stimulation site. If this intensity did not elicit any

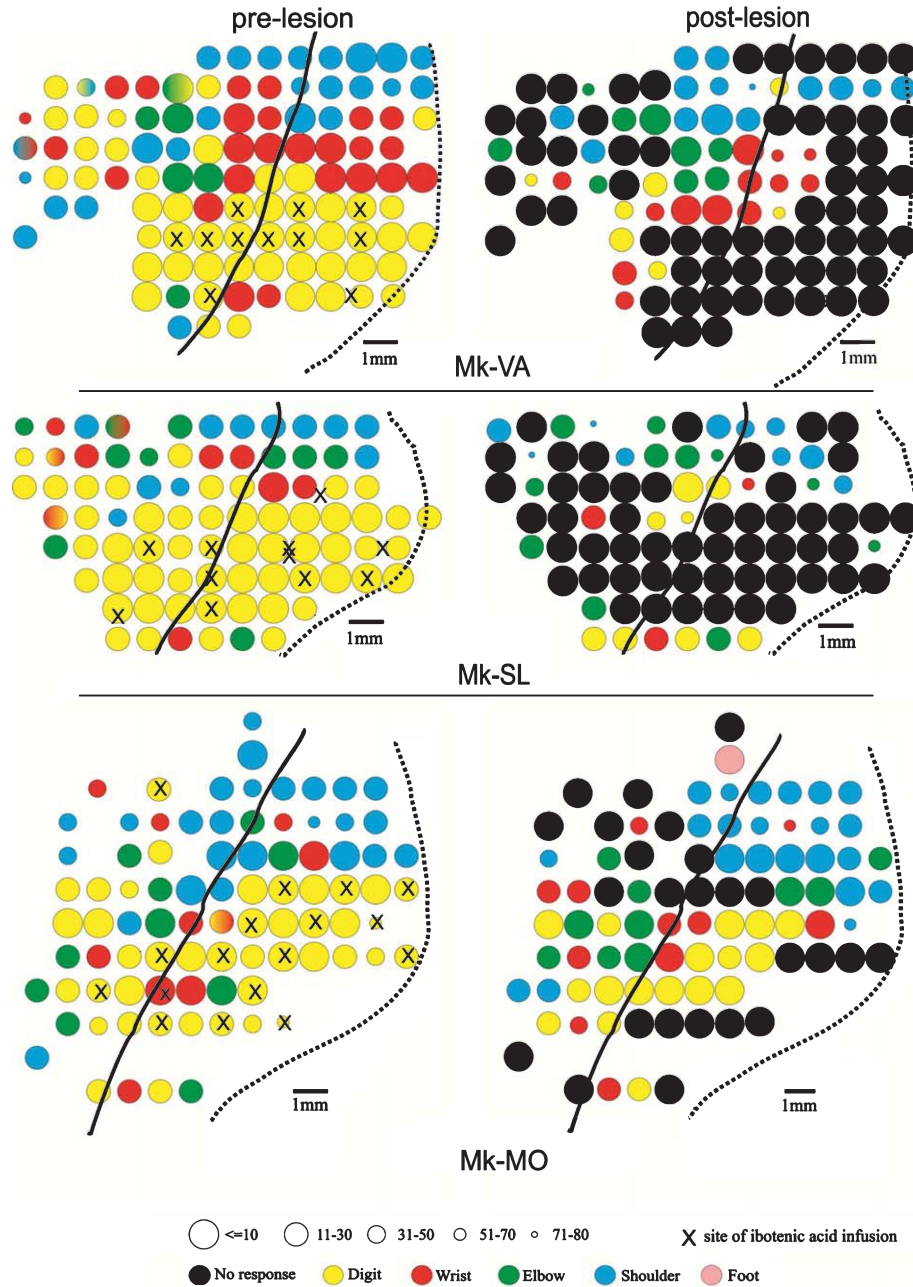


Fig. 3. Unfolded ICMS maps established pre-lesion (left column) and post-lesion (right column) in the three anti-Nogo-A antibody treated monkeys Mk-VA, Mk-SL and Mk-MO. Same conventions as in Fig. 1.

movement, then it was progressively increased until threshold, but not above 80 microamps (in the absence of response at 80 microamps, the site was considered as non-responsive). On the other hand, if the slightly increased intensity produced an effect, then it was

decreased until threshold. During the entire stimulation period at each ICMS site, one experimenter held the monkey's forelimb and passively moved it to different postures to determine the effect of the ICMS on the different joints (fingers, wrist, elbow, shoulder, etc).

## 2.6. Cortical lesion and anti-Nogo-A antibody pump implant

In each monkey, after completion of the ICMS map and precise delineation of the hand representation in M1, as well as some behavioral retraining, a permanent lesion of M1 was performed unilaterally, targeted to the hand area. The cortical lesion was produced by infusion of ibotenic acid (Sigma) at multiple sites (Table 1), where movements of the fingers were obtained at low threshold in response to ICMS. The precise procedure of ibotenic acid infusion was described earlier (Liu and Rouiller, 1999; Kaeser et al., 2010; Hamadjida et al., 2012). In a separate and recent study, the time-course of the neurotoxic effect of ibotenic acid infusion in the cerebral cortex of a monkey was assessed based on cerebral blood flow and MRI measurements (Peuser et al., 2011). A volume of 1  $\mu$ l to 1.5  $\mu$ l of ibotenic acid solution (10  $\mu$ g/ $\mu$ l phosphate buffer saline) was injected at each selected ICMS site, via a 10  $\mu$ l Hamilton syringe replacing the electrode at the corresponding penetration site. The total volume of infusion was adapted to the extent and shape of the hand representation in M1 previously determined by ICMS. Ibotenic acid is expected to diffuse approximately 1.5 mm around the center of injection site (by analogy with diffusion of muscimol; see Martin, 1991). The distance between adjacent infusion sites thus ranged between 1.5 to 3 mm, in order to cover most of the hand representation. In the initial monkeys (Table 1: Mk-CE and Mk-JU), the infusion of ibotenic acid took place when the animal was awake and sat quietly in the primate chair. A few minutes after infusion of ibotenic acid, a progressive motor deficit of the contralateral hand appeared, reflected by a flaccid paralysis of the hand. In subsequent monkeys (Table 1), ibotenic acid was injected under anaesthesia.

On the day of the lesion, the monkeys subjected to a lesion of M1 were separated into two groups (Table 1). One group of five monkeys did not receive any treatment (control monkeys) whereas the second group of three monkeys was treated with the anti-Nogo-A antibody 11C7 (Oertle et al., 2003). The treated monkeys were implanted in the neck region (in a subcutaneous pouch), under deep anaesthesia, with two osmotic pumps (Alzet<sup>®</sup>, model 2ML2, 5  $\mu$ l/h), containing the anti-Nogo-A antibody 11C7 at a concentration of 3 mg/ml. One osmotic pump was used to infuse the antibody intrathecally in the spinal cord at cervical level, as previously reported in our studies on

spinal cord injury (Freund et al., 2006, 2007, 2009). The second osmotic pump was used to deliver the anti-Nogo-A antibody at cortical level, close to the lesion territory. The catheter of this second osmotic pump was tunnelled under the skin to the head of the monkey. Through a small opening in the skull, the tip of catheter was pushed under the dura in close proximity to the motor cortex. Once the catheters from both osmotic pumps were in place, the muscles and skin were sutured. The osmotic pumps delivered the antibody treatment during 4 weeks and then they were removed under deep anaesthesia. The untreated monkeys were not implanted with osmotic pumps.

## 2.7. Processing of ICMS data: Unfolding the motor cortex maps

ICMS data were represented in two different types of cortical maps: a standard (raw) ICMS map (see Liu and Rouiller, 1999; Kaeser et al., 2010: Supplemental Fig. 1 panel A) and an unfolded ICMS map (see Park et al., 2001, 2004; Kaeser et al., 2010: supplemental Fig. 1 panel C). The standard ICMS map consisted in projecting the lowest ICMS threshold obtained along an individual electrode track on the surface of the motor cortex, at the location of electrode penetration. The resulting ICMS map forms a grid with intervals of 1 mm  $\times$  1 mm and allows ICMS positioning on the brain surface (Fig. 1A). The limitation of this method is that electrode tracks running in the rostral bank of the central sulcus in parallel to the cortical layers is represented only by a single point on the surface, although the electrode may have stimulated layer V neurons at low threshold at several adjacent sites (see Kaeser et al., 2010: Supplemental Fig. 1). In contrast, the unfolded map represents all sites, including numerous ones in the rostral bank of the central sulcus, where the lowest thresholds were obtained by ICMS, presumably at the location of abundant pyramidal cells in layer V. This is in line with tracing data showing a high density of corticomotoneuronal cells in the rostral bank of the central sulcus (He et al., 1993, 1995; Rathelot and Strick, 2006). As a consequence, the multiple ICMS sites in layer V encountered along an individual electrode track in the rostral bank of the central sulcus appear in the unfolded ICMS map (see Kaeser et al., 2010: Supplemental Fig. 1). In summary, a two-dimensional rendering of cortical layer V in the rostral bank of the central sulcus required flattening and unfolding of its curvature. To this aim, all electrode tracks were first grouped

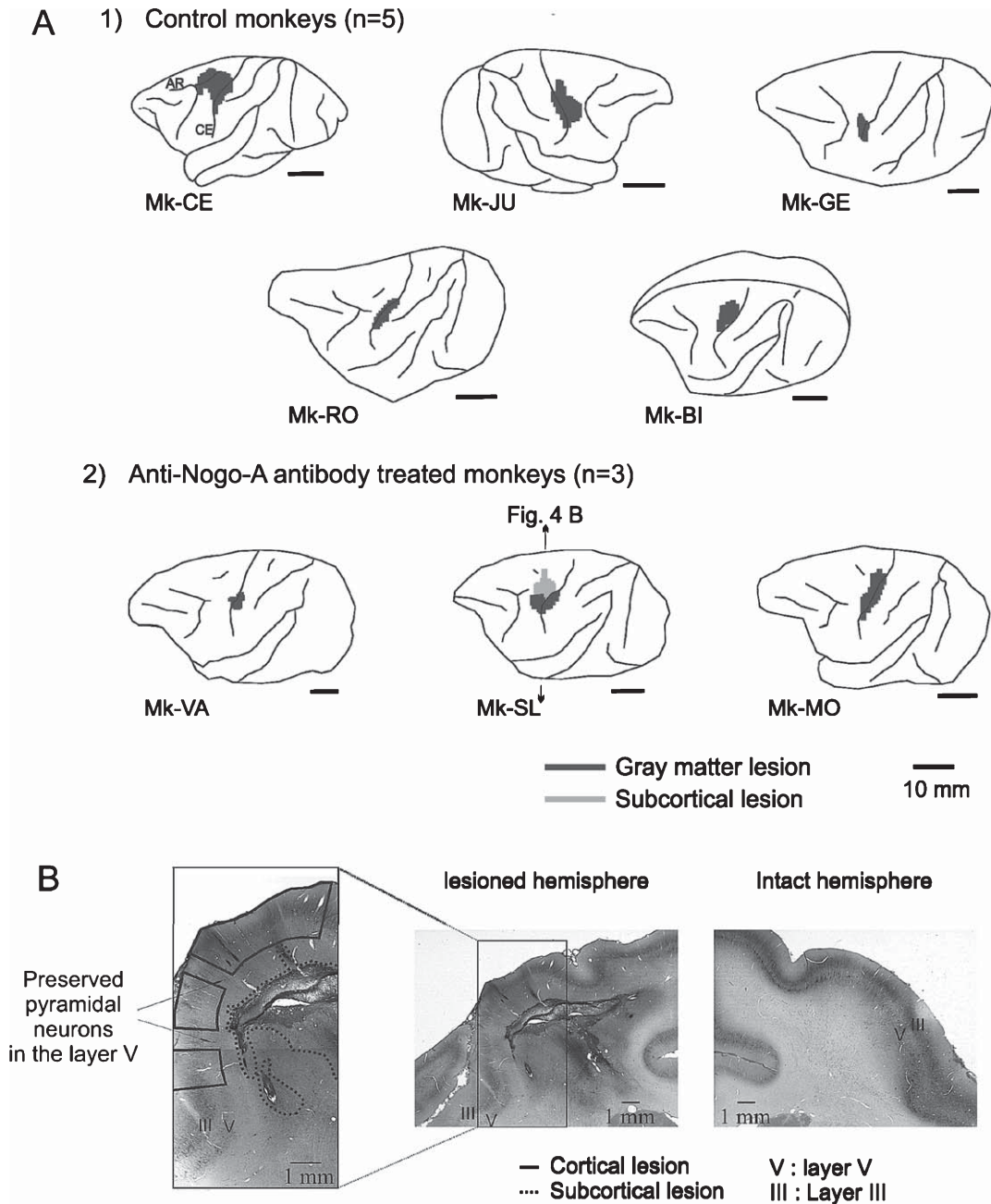


Fig. 4. Panel A: Lateral views, for control (1) and anti-Nogo-A antibody treated (2) monkeys, on the surface of the corresponding hemisphere of the lesion extent in the gray matter area (black area) and in subcortical area (gray area) for one monkey in the motor cortex, as seen in transparency of the cortical surface (same data as shown previously for some monkeys in Kaeser et al., 2010, 2011; Bashir et al., 2012; Hamadjida et al., 2012). The surface representation of the lesion does not reflect directly the actual volume of the gray matter territory impacted by the infusion of ibotenic acid (see for that Table 1 and Figs. 9 and 10). Panel B: View of SMI-32 staining in Mk-SL, showing the 2 hemispheres on a frontal histological section of the brain, at low magnification (middle and right pictures). In the intact hemisphere, the layer V containing the corticospinal neurons is continuous in the motor cortex all along its medio-lateral extent. In contrast, in the lesioned hemisphere, as shown on the left at higher magnification, three territories exhibit an interruption of the layer V, corresponding to cortical zones affected by the ibotenic acid injections (each delineated with a solid line). Note also the presence of a subcortical lesion outlined with a dashed contour, and corresponding to the gray zone displayed in panel A (2), for Mk-SL.

according to their medio-lateral coordinate. Within each group, the tracks were then ordered according to their rostral-caudal coordinate. On the basis of electrophysiological data and observations, a parasagittal diagram was constructed to represent the cortex that was explored and stimulated. The white matter was identified by a sharp increase of the ICMS effective intensity or even a loss of effect of ICMS on the forelimb joints. The reconstruction of the position of the precentral sulcus was based on the successive ICMS sites that produced effects at the lowest threshold, and the sensory cortex was identified by the absence of forelimb movement or by a significant increase of the ICMS effective intensity, mostly in the fundus of the central sulcus. For each electrode track, sites corresponding to cortical layer V were identified using a combination of electrode depths, and the lowest threshold ICMS intensity site. Electrode penetrations on the convexity of the precentral gyrus traversed cortical layers perpendicularly and, in such cases, it was relatively easy to identify the ICMS site closest to layer V, corresponding to the lowest threshold. For electrode penetrations running along the rostral bank of the central sulcus, roughly parallel to the cortical layers, it was more difficult to identify layer V sites. In such cases, output effects from sites at the same depth from different electrode tracks along the rostral-caudal axis were compared. This analysis yielded a series of reconstructed parasagittal cortical sections oriented along the rostral-caudal axis of the chronic chamber in the plane of the electrode tracks. The first ICMS site of the identified convexity of the rostral bank of the central sulcus was used as the axis for rotating and unfolding the layer V (see Kaeser et al., 2010: Supplemental Fig. 1).

### 2.8. *Histological processing*

As previously reported (Kaeser et al., 2010), at the end of the experiments (after completion of pharmacological investigations and tracer injections: see Hamadjida et al., 2012 and Hoogewoud et al., 2013), the monkeys were euthanized with an overdose of pentobarbital sodium (90 mg/kg body weight; i.p.). Trans-cardiac perfusion with 0.9% saline (500 ml) was followed by a solution of fixative (4,000 ml of 4% phosphate-buffered paraformaldehyde) and solutions of sucrose (10, 20, 30% in paraformaldehyde). The brains were soaked in a 30% solution of sucrose (in phosphate buffer) for cryo-protection for a few days. Frontal sections (50  $\mu$ m thick) of the brain were cut

using a cryostat and collected in five series. One series of sections was Nissl stained with cresyl violet, whereas a second series was processed to visualize the marker SMI-32, as previously described (Beaud et al. 2008; Liu et al., 2002; Wannier et al., 2005). The Nissl and SMI-32 consecutive series of sections were used to reconstruct the position and extent of the permanent lesion in the cerebral cortex. The SMI-32 stained sections displayed the pyramidal neurons in layers III and V (Fig. 4B). Finally, the lesion was transposed onto a lateral view of the cortical surface of the lesioned hemisphere (Fig. 4A). Using a specific tool of the NeuroLucida software (based on the Cavalieri method; see e.g., Pizzimenti et al., 2007), the volume of the cortical lesion (in mm<sup>3</sup>) affecting the cortical gray matter was calculated by extrapolation from the reconstructions of the lesion on consecutive histological sections of the brain taken at 0.25 mm interval (Table 1).

## 3. Results

### 3.1. *Monkeys involved in the present study*

The present data were collected from eight monkeys, already included in recent reports from this laboratory, related to the performance of the ipsilesional hand after M1 lesion (Kaeser et al., 2010; Bashir et al., 2012), or used as control ( $n=5$ ) in a preliminary approach to establish a cell therapy based on implantation of autologous adult progenitor cells (Kaeser et al., 2011), or aimed at investigating the changes of callosal connectivity in relation to the M1 lesion and the anti-Nogo-A antibody treatment (Hamadjida et al., 2012). Some of these animals were also used to pharmacologically investigate the role played by the ipsilesional premotor cortex (PM) in functional recovery (Hoogewoud et al., 2013). In all of these studies, the ID codes used for the monkeys are the same and therefore they can be easily identified in each individual report. In the present study, the eight monkeys subjected to M1 lesion were specifically analyzed to address the issue of motor map changes using ICMS (Table 1), representing the new contribution of the current report.

The permanent lesion in the motor cortex, resulting from ibotenic acid injections, were illustrated with corresponding views in SMI-32 and Nissl staining histological material in previous reports (Kaeser et al., 2010; Peuser et al., 2011). Another example is shown here in Fig. 4B (SMI-32 staining), derived from Mk-

SL. The lesion territories are characterized by an interruption of the layer V, which contains when intact the pyramidal neurons stained with SMI-32, corresponding to the corticospinal neurons. In between the three lesion areas, there are two zones in which the layer V still contains SMI-32 positive neurons, thus corresponding to small territories spared by the lesion.

### 3.2. Pre-lesion motor maps

In all monkeys, before the lesion of M1, ICMS experiments were conducted to delineate the hand representation in M1, defined as the cortical sites where ICMS elicited movements of the digits of the contralateral hand at the lowest threshold. After approximately 1–2 months of daily ICMS sessions, a raw cortical motor map was obtained (Fig. 1A; as illustrated in Mk-BI), showing the position on the cortical surface of the electrode penetrations. The hand area on the cortical surface corresponds to the sites of electrode penetrations along which the ICMS effect observed at the lowest threshold was a movement of digits of the contralateral hand (yellow circles in Fig. 1A). As expected, ICMS delivered at more medial and/or rostral electrode penetrations elicited at lowest threshold movement of more proximal body territories (wrist, elbow, shoulder) and/or face muscles or foot (Fig. 1A). To avoid damage of the cerebral cortex as might be induced by too many electrode penetrations, the ICMS was mostly focused on the hand representation in M1, without extensive mapping of either the adjacent motor cortical areas (PM, SMA) or of the other body territories in M1 (e.g. face, trunk, leg, etc).

A first analysis of these raw data aimed at obtaining a more comprehensive representation of the motor map focused on the hand representation by unfolding the central sulcus (mostly the rostral bank of the central sulcus, as explained in the methods: Fig. 1B). In the rostral bank of the central sulcus (where the hand representation is mostly located), the electrode penetrations are roughly parallel to the cortical layers. Consecutive ICMS sites eliciting digit movements at low threshold are encountered along the same electrode penetration (presumably following layer V), thus corresponding to an enlargement of the hand area (yellow circles) in the caudal direction (Fig. 1B in the same Mk-BI), as compared to the raw motor map (Fig. 1A). Similarly unfolded pre-lesion motor maps have been established for the other seven monkeys (left column in Figs. 2 and 3). In the unfolded map pre-lesion, only the ICMS

responsive sites were considered. These data show that the extent of the hand area, as delineated by ICMS, is quite variable across monkeys (see Table 1: estimates of “unfolded” hand area). As expected for M1, most ICMS sites elicit corresponding body movements at low intensity (below 10 microamps).

The “x” symbols in the pre-lesion unfolded motor maps represent the ICMS sites selected for infusion of ibotenic acid to generate a permanent chemical lesion of the hand representation in M1. The reconstruction of the lesion, as seen on a lateral view of the cerebral cortex, is represented in Fig. 4A for each of the eight monkeys included in the present study. The volume of the lesion territory has been assessed (Table 1), from histological sections treated for the marker SMI-32, as previously reported in detail (Kaeser et al., 2010; Bashir et al., 2012; Hamadjida et al., 2012).

Starting a couple of days after the lesion, the behavioral sessions were pursued, as before lesion, to assess manual dexterity. As a result of unilateral ibotenic acid infusion in the hand area in M1, the contralateral hand was paralyzed, corresponding to a score of zero in all manual tests (see Liu and Rouiller, 1999; Kaeser et al., 2010, 2011; Schmidlin et al., 2011; Bashir et al., 2012; see Fig. 8A for the 3 treated monkeys). During the following weeks, there was a progressive recovery of manual dexterity, reaching a post-lesion plateau of manual performance. In most cases, the extent of functional recovery is incomplete (Table 1). After the post-lesion plateau of manual performance has been established for several weeks or months, a second series of ICMS sessions took place to determine the post-lesion motor map in the cortical area in and around the lesion. The time interval between the lesion of the motor cortex (ibotenic acid infusion) and the onset of the second ICMS mapping is indicated in Table 1 for each monkey.

### 3.3. Post-lesion motor maps

Post-lesion, the very same ICMS sites as in the unfolded pre-lesion map were re-visited, when the monkeys reached a post-lesion plateau. The unfolded ICMS maps established post-lesion (panel C in Fig. 1 and right columns in Figs. 2 and 3) appear very different from the pre-lesion unfolded ICMS maps. As expected for a permanent lesion induced by ibotenic acid infusion, a majority of territories became non-responsive to ICMS (black circles in Fig. 1C, right column in Figs. 2 and 3), in spite of high intensity

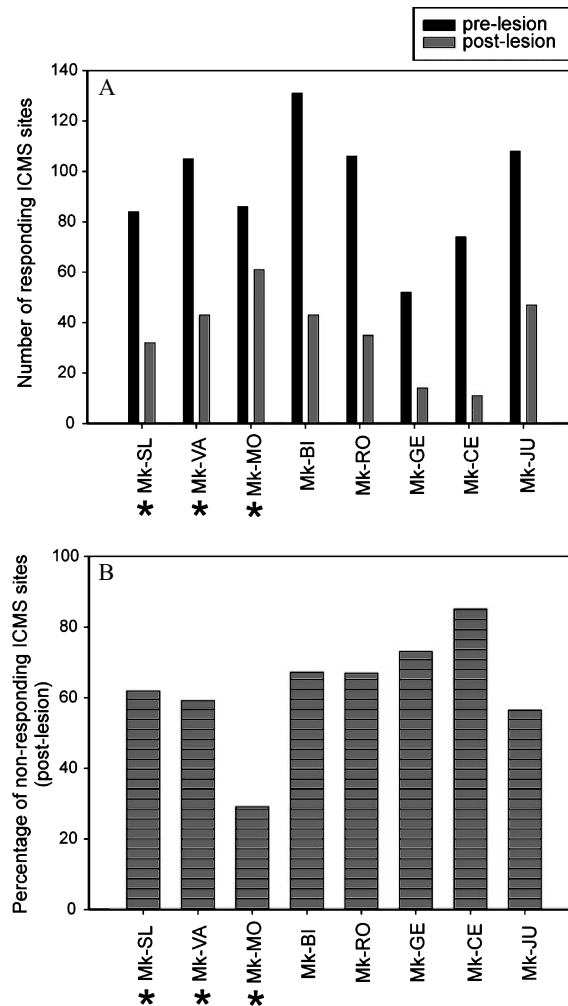


Fig. 5. A: Comparison pre- versus post-lesion for each monkey of the number of ICMS responsive sites (effect on joints elicited at an intensity lower than 80 microamps). B: Derived from panel A, the bar graphs show for each monkey the percentage of ICMS sites which became non-responsive as a result of the lesion in the motor cortex. In the two panels, the three monkeys on the left (asterisks) were subjected to anti-Nogo-A antibody treatment whereas the five monkeys on the right were control (untreated).

stimulation (up to 80 microamps). In one monkey (Mk-CE; Fig. 2), none of the pre-lesion sites where ICMS elicited digit movements were preserved by the lesion: the entire previous hand area was replaced post-lesion by a non micro-excitable territory (except at 2 sites, replaced by an effect on foot muscles). In Mk-JU, in the post-lesion ICMS map, there was a replacement of hand sites either by a non micro-excitable territory or by more proximal body territories, such as wrist, shoulder or even foot (Fig. 2). In all other monkeys (Figs. 1–3), a large proportion of ICMS sites belonging to the hand area pre-lesion became non-responsive post-lesion. However, in these monkeys (Mk-GE, Mk-

VA, Mk-SL, Mk-RO, Mk-BI, Mk-MO, in increasing order), there were ICMS sites still eliciting digit movements at the lowest threshold along the corresponding electrode track. In parallel, in these monkeys, some other ICMS sites eliciting digit movements pre-lesion were replaced by more proximal muscle territories (Figs. 1–3). Overall, out of eight monkeys, the change of ICMS map post-lesion of the motor cortex was quite variable from one animal to the next. With extremely rare exceptions (one site in Mk-VA, one site in Mk-GE) none of the ICMS sites located pre-lesion clearly outside the hand area (e.g. proximal territory) was changed post-lesion into an ICMS site eliciting digit move-

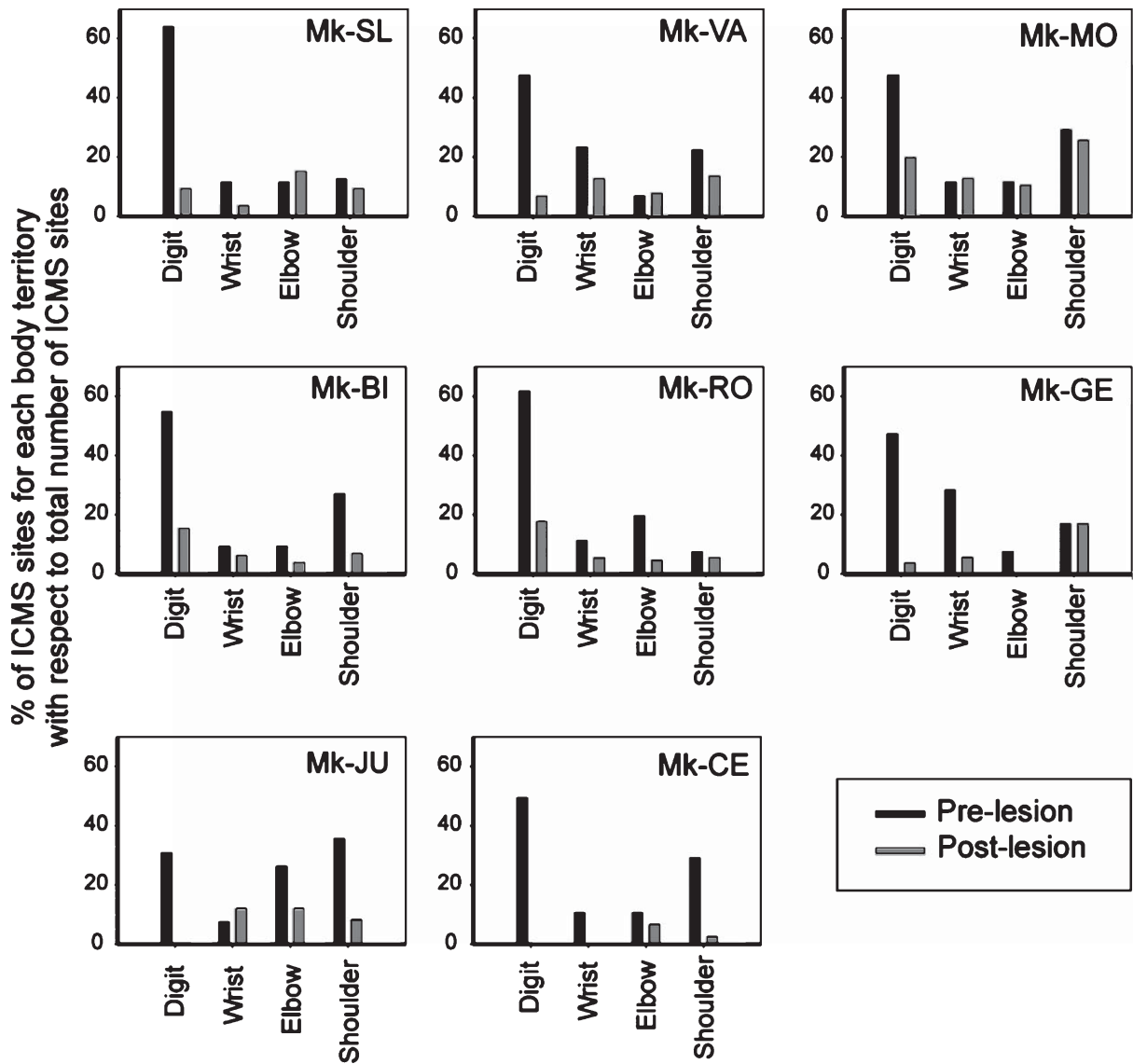


Fig. 6. For each monkey, the histograms show the distribution of the ICMS sites in M1 with respect to the body territory (forelimb), at which the current at threshold elicited a movement before the lesion of M1 (black bars). In each graph, the sum of the four black bars is 100%. The grey bars show the distribution of the same ICMS sites post-lesion, showing that a large proportion of ICMS sites became non-responsive (only the responsive ICMS sites post-lesion have been distributed; their sum is thus clearly smaller).

ments. On the other hand, when digit ICMS sites were present post-lesion, it was in general at a site that was already devoted to the hand area pre-lesion (Figs. 1–3).

### 3.4. Comparison of ICMS data pre-lesion versus post-lesion

The number of sites where ICMS was applied pre-lesion was quite variable from one monkey to the next

and this is not a meaningful parameter. In contrast, as the very same ICMS sites were re-visited post-lesion, comparing this initial number to the number of still responding sites post-lesion provides a valuable assessment of ICMS map changes (Fig. 5). In all monkeys, there was a substantial decrease of responding ICMS sites post-lesion (Fig. 5A), though to a quite variable extent across animals, better seen when plotting the percent of non-responsive ICMS sites post-lesion with

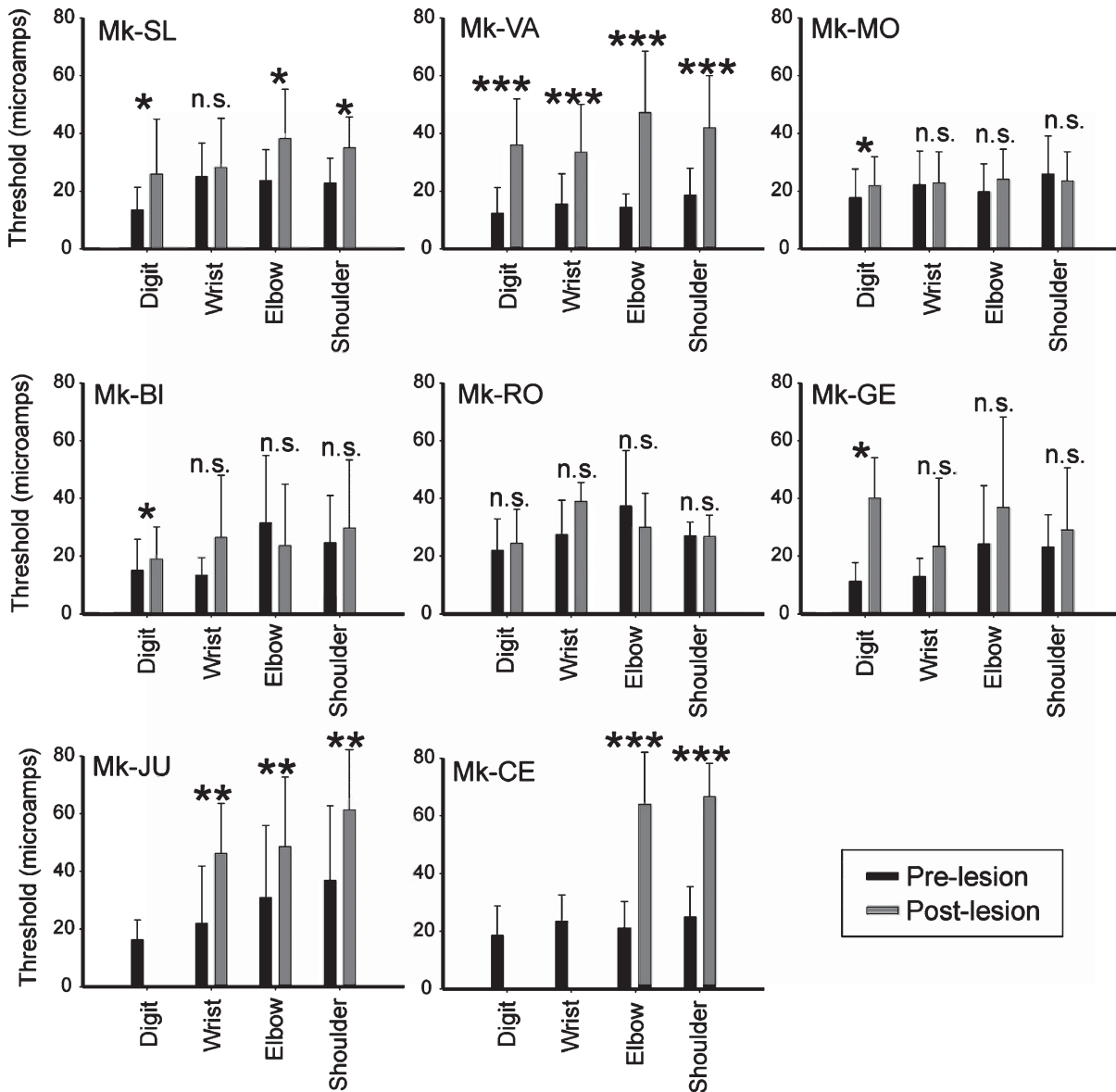
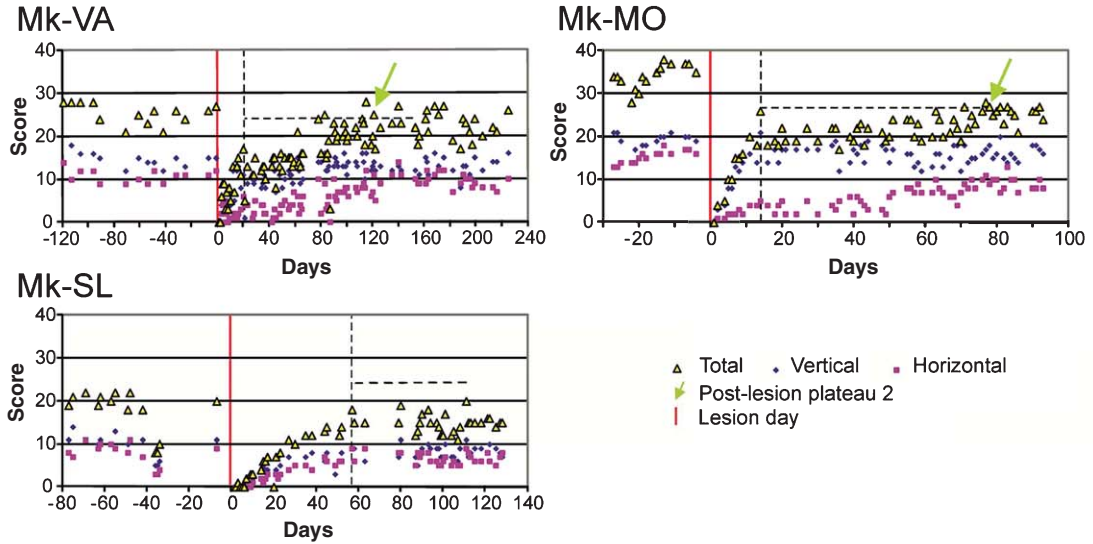


Fig. 7. For each monkey, the histograms show the distribution of the ICMS threshold values at which the effect was observed, pre-lesion (black bars) and post-lesion (grey bars). For each body territory (forelimb), the bars indicate the mean threshold and the standard deviation (SD). Note a general increase of threshold post-lesion as compared to pre-lesion. The number of ICMS sites considered post-lesion is much smaller than pre-lesion, as the majority of ICMS sites became non-responsive post-lesion (see Figs. 1–3; 5–6). The distributions of thresholds were compared pre- versus post-lesion in each monkey and for each territory (e.g. digit, wrist, etc), using the Mann and Whitney test: n.s. (not statistically significant) is for  $p > 0.05$ ; \*  $p < 0.05$ ; \*\*  $p < 0.01$ ; \*\*\*  $p < 0.001$ .

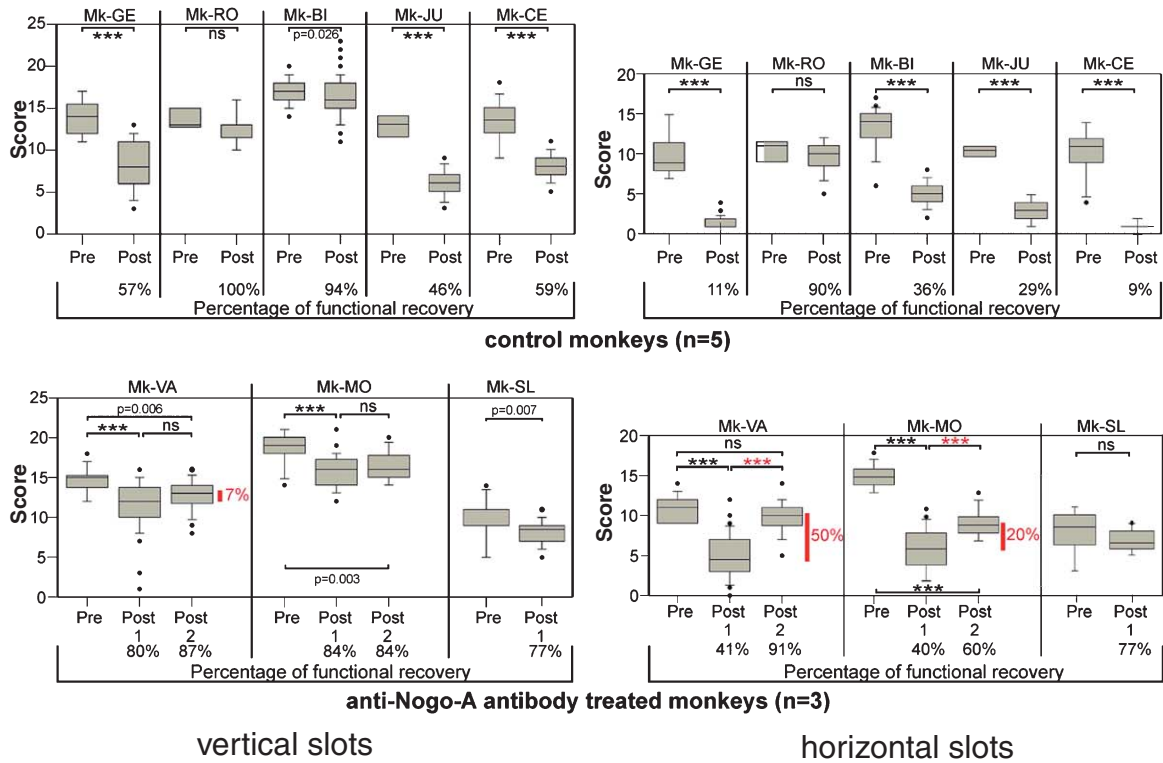
respect to the total number of responding sites pre-lesion (Fig. 5B). The percentage of non-responding ICMS sites ranged from 29% to 85%, in line with the relatively high number of black circles in Figs. 1–3. In Fig. 6, for each monkey, the bar graphs in black show the pre-lesion percent distribution of ICMS sites with

respect to the corresponding body territories activated: as expected, as the goal of the ICMS sessions was to delineate the hand representation, the majority of ICMS sites elicited digit movements at threshold. The gray bar graphs in Fig. 6 show the same percent distribution but post-lesion, for the sites which still elicited

**A** Score of manual dexterity in Modified Brinkman board task for anti-Nogo-A antibody treated monkeys (n=3)



**B** Comparison of scores pre- versus post-lesion



a motor response. The percent of digit sites decreased dramatically or even totally disappeared (Mk-JU and Mk-CE). For nearly all other territories, there was also a decrease of responding sites, but generally to a lesser extent than for the digits. This observation suggests that the infusion of ibotenic acid in the hand representation also exerted a detrimental effect at some distance, either by diffusion of the neurotoxic drug and/or indirectly by affecting local networks.

Due to the motor cortex lesion, one would expect that the ICMS sites still present after the lesion in the ICMS map elicit movements at a higher threshold than pre-lesion. This prediction has been largely confirmed by the present experiments, as illustrated in Fig. 7. The increase of ICMS threshold was statistically significant for all body territories in monkeys Mk-VA, Mk-JU, Mk-CE and, except for the wrist, in Mk-SL. In three other monkeys (Mk-MO, Mk-BI and Mk-GE), the increase of threshold was statistically significant only for the digits. Finally, in the monkey with the smallest lesion (Mk-RO), there was no statistically significant increase of threshold post- versus pre-lesion. In only three cases (Mk-BI, Mk-RO and Mk-MO), the threshold was lower post-lesion than pre-lesion for the elbow territory in the first two monkeys and in the shoulder territory for the latter, but in all three cases the difference was not statistically significant. When present, the extent of the threshold increase post- versus pre-lesion was again quite variable from one monkey to the next (Fig. 7).

### 3.5. Behavioral data

Based on the modified Brinkman board task, manual dexterity was assessed by the number of pellets

(score) retrieved during the first 30 seconds (Schmidlin et al., 2011) on each daily behavioral session. In contrast to our recent report (Kaeser et al., 2011) focused on the total number of pellets retrieved (total score), the score data were analyzed here separately for the vertical slots and the horizontal slots. Plots of the behavioral performance of the three anti-Nogo-A antibody treated monkeys are shown in Fig. 8 (panel A). Before the lesion, after an initial training phase (not shown), the monkeys reached a generally stable manual performance, reflected by a pre-lesion plateau of score. Immediately after the lesion, as expected, the manual dexterity of the contralesional hand dropped to zero. After the lesion, a progressive functional recovery took place during several weeks, to reach a post-lesion plateau. The beginning of the post-lesion plateau (vertical dashed line in panel A of Fig. 8), was determined based on criteria as defined in Kaeser et al. (2011). In two out of the three anti-Nogo-A antibody treated monkeys (Mk-MO and Mk-VA), there was a rebound of score, with a subsequent (significant) increase in the number of pellets retrieved, initiated on the day pointed out by the green arrow (see Kaeser et al. 2011, for criteria to define the onset of the rebound). The same, original plots of score, showing the deficit immediately after the lesion and the subsequent (spontaneous) functional recovery in the five control monkeys, have been published in recent reports (Kaeser et al., 2010, 2011; Bashir et al., 2012). These plots showed that, in the five control monkeys, there was no such rebound of score post-lesion, as observed in Mk-VA and Mk-MO (panel A in Fig. 8). The ratio of the post-lesion plateau score (median value) to the pre-lesion plateau score (median value) defines the percentage of functional recovery, computed for each monkey separately for vertical and

Fig. 8. **A:** Behavioral data for the three monkeys subjected to anti-Nogo-A antibody treatment, showing the manual dexterity performance (score) in the modified Brinkman board task, as a function of time corresponding to daily sessions pre-lesion (negative days) and post-lesion (positive days). The vertical red line represents the day of M1 lesion. Note the dramatic drop of manual dexterity immediately after the lesion of M1. The score (number of pellets retrieved in 30 seconds) is given for the vertical slots (blue diamonds), the horizontal slots (red squares), whereas the yellow triangles are for the total score (sum of vertical and horizontal slots). As described earlier (Kaeser et al., 2010), the vertical dashed line points to the onset of a first post-lesion plateau, most likely reflecting the “spontaneous” functional recovery level. The horizontal dashed line shows an upper limit of score given by the median value at first plateau plus twice the difference between the median value and the highest value at plateau. In two monkeys (Mk-VA and Mk-MO), the score reached this upper limit (green arrow) later during the post-lesion phase, interpreted as a second plateau or rebound of functional recovery, possibly reflecting the effect of the anti-Nogo-A antibody treatment. The same plots were presented earlier for the five control monkeys (Kaeser et al., 2011) and showed that none of the control monkeys exhibited such a rebound of functional recovery. **B:** Comparison in the form of box and whiskers plots of pre-lesion (“Pre”) and post-lesion (Post 1) scores in the five control monkeys (top panels) and in the three anti-Nogo-A antibody treated monkeys, separately for the vertical slots (left) and the horizontal slots (right). In the two monkeys with a rebound of functional recovery, the middle box is for the first post-lesion plateau (Post 1) and the rightmost box is for the second post-lesion plateau (Post 2). The percent values in red are for the enhancement of functional recovery obtained by reaching the second plateau as compared to the first post-lesion plateau. In the Mann-Whitney test, comparison between pre-lesion and post-lesion median values (first or second plateaux), \*\*\*  $p < 0.001$ , whereas “n.s.” is for not significant ( $p > 0.05$ ).

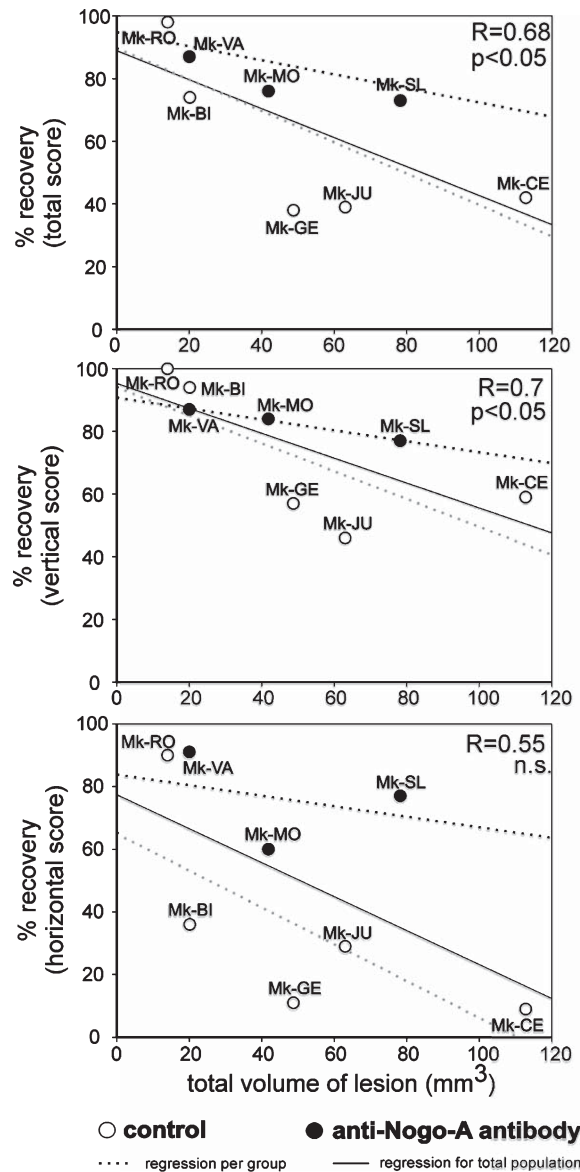


Fig. 9. Scatter plots of functional recovery (in percent) as a function of the volume of the lesion in the motor cortex (in mm<sup>3</sup>), for the total score (top panel), the vertical slots (middle panel) and the horizontal slots (bottom panel). Control monkeys are represented by empty symbols whereas filled circles are for the anti-Nogo-A antibody treated monkeys. The regression line was calculated for all data points, reflecting the general trend towards a decrease of functional recovery for increasing lesion sizes, as expected. Coefficients of correlation are given in the upper right corner of each plot, with the corresponding *p* value. Regression lines for each group are indicated by dashed lines.

horizontal slots, as illustrated in the form of box and whisker plots in Fig. 8 (panel B; see also Table 1). In the five control monkeys, the degree of functional recovery ranged between 46% and 100% for the vertical slots and between 9% and 90% for the horizontal slots. Taking into account the final second plateau post-lesion in Mk-VA and Mk-MO, the degree of functional recovery

among the three anti-Nogo-A antibody treated monkeys ranged between 77 and 87% for the vertical slots and between 60 and 91% for the horizontal slots.

In order to illustrate the benefit provided by the second post-lesion plateau, reflecting a rebound of functional recovery as observed in the anti-Nogo-A

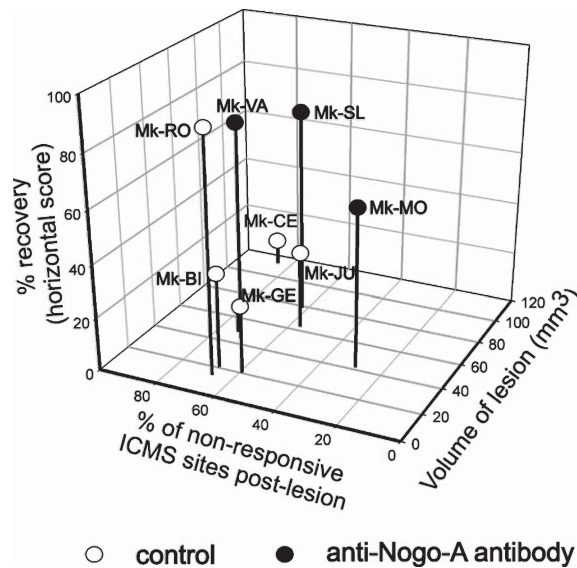


Fig. 10. 3D scatter plot showing the relationship between the degree of functional recovery (in %), the volume of the lesion (in mm<sup>3</sup>) and the percent of non-responsive ICMS sites.

antibody treated monkeys Mk-VA and Mk-MO, video sequences are shown at the following URL address: <http://www.unifr.ch/neuro/rouiller/FRJS/index.html>. In a control monkey (Mk-BI), three video sequences illustrate the manual dexterity of the monkey before lesion, in the acute phase (immediately post-lesion) and finally at the level of the unique post-lesion plateau (see also Fig. 8B). Immediately post-lesion, Mk-BI lost the ability to retrieve pellets with the contralesional (right) hand and therefore cheated by trying to use the left hand. At the level of the post-lesion plateau, Mk-BI recovered the manual dexterity to some extent, but mainly for the vertical slots which were preferentially aimed for, with fairly good success before aiming for the horizontal slots with much more difficulty and error occurrences (pellet pushed to neighbouring slots). As expressed by the score (number of pellets retrieved during the first 30 seconds of the test), the degree of functional recovery was more prominent for the vertical slots (94%) than for the horizontal slots (36%; see Fig. 8B). In contrast, in the anti-Nogo-A antibody treated monkey Mk-VA, functional recovery occurred into two phases (first and second post-lesion plateau; see Fig. 8A and B), with a comparable percentage of functional recovery for the vertical (87%) and the horizontal (91%) slots. The video sequences for Mk-VA also show the dramatic loss of manual dexterity immediately post-lesion,

as compared to pre-lesion. In that case, in the acute phase, Mk-VA also tried to cheat by using the left hand, instead of the contralesional (right) hand. The two video sequences taken at post-lesion plateaux illustrate qualitatively the manual performance at the first (video sequence 3) and second post-lesion (video sequence 4) plateau, respectively. At post-lesion plateau 2, the same monkey Mk-VA was obviously more dextrous than at post-lesion plateau 1. At the latter (video sequence 3), Mk-VA focused on the vertical slots first, at a relatively slow pace, before aiming at the horizontal slots with great difficulty and several errors. At the second plateau (video sequence 4), Mk-VA aimed for both vertical and horizontal slots from the onset of the test, at a much higher pace for both slot orientations. Whilst Mk-VA completed the modified Brinkman board at the second plateau (all 50 slots emptied), for comparison, at first plateau, after the same amount of time, this monkey only emptied 28 out of 50 slots. Moreover, at the second post-lesion plateau (video sequence 4), Mk-VA scanned the Brinkman board more systematically than at the level of the first post-lesion plateau (video sequence 3). This comparison of video sequences 3 and 4 for Mk-VA thus emphasizes the substantial benefit provided by the rebound of functional recovery up to the second plateau, as observed for the 2 anti-Nogo-A antibody treated monkeys Mk-VA and Mk-MO.

The variability of the degree of functional recovery within the two subgroups of monkeys is related, at least in a large part, to the size of the cortical lesion. For this reason, the degree of functional recovery in percent was plotted as a function of the volume of the cortical lesion (Fig. 9). As expected, considering all eight monkeys, there was a general trend towards a decrease of functional recovery as a result of increasing lesion size (see regression lines in Fig. 9). First of all, the control monkey Mk-RO with the smallest lesion exhibited an excellent spontaneous functional recovery. Looking at the vertical slots data (middle panel in Fig. 9), the distribution of functional recovery for the control monkeys was fairly comparable to that obtained for the anti-Nogo-A antibody treated monkeys. In sharp contrast, the functional recovery was distributed in a clearly more disparate way when considering the horizontal slots (bottom panel in Fig. 9). As grasping from the horizontal slots is more challenging than from the vertical slots (see Freund et al., 2009; Schmidlin et al., 2011), the deficit in control monkeys is more prominent whereas, in the anti-Nogo-A antibody treated monkeys, the treatment resulted, irrespective of the lesion volume, in a substantial restitution of this sophisticated manual ability (combination of precision grip and arm pronation or supination movement needed for grasping from the horizontal slots). In more detail, the anti-Nogo-A antibody treated monkey Mk-VA with a larger lesion recovers the ability to grasp from the horizontal slots a bit more than the control monkey Mk-RO which displays a smaller lesion (bottom panel in Fig. 9). The two anti-Nogo-A antibody treated monkeys Mk-MO and Mk-SL recovered clearly better than the other control monkeys (bottom panel in Fig. 9). As expected, the plot based on the total score (sum of vertical and horizontal slots; top panel in Fig. 9) yields an intermediate figure between the two slot orientations taken separately. The difference between the two groups of monkeys with respect to functional recovery is reflected by their respective regression lines (Fig. 9), again with a more prominent difference observed for the horizontal slots than for the vertical ones.

To address the question of whether the functional recovery may also be correlated to the change of motor maps in M1 (in and around the lesion territory), the three parameters percent of functional recovery for horizontal slots, volume of lesion and the percentage of non-responsive ICMS sites post-lesion were plotted in 3D form (Fig. 10). It appears that the two subgroups of monkeys, differing to some extent with

respect to the percentage of functional recovery (except the control monkey Mk-RO with the smallest lesion), superimpose to a large extent as far as the percentage of non-responsive ICMS sites is concerned. In other words, the number of ICMS sites in M1 still eliciting forelimb movements is a poor predictor of the functional recovery for the horizontal slots, which is a more sensitive parameter than the vertical slots. There is also overlap between the two subgroups of monkeys with respect to the volume of the cortical lesion.

#### 4. Discussion

The results of the present study can be summarized as follows: 1) after permanent chemical lesion of the hand area in M1 in the adult macaque monkey, the lesion territory becomes mostly non micro-excitable several months post-lesion, in spite of some functional recovery (spontaneous or promoted by anti-Nogo-A antibody treatment); 2) some sites within the lesion territory remain excitable, but independent of the degree of functional recovery; 3) around the lesion in M1, there was no evidence for a reallocation of proximal territories to distal functions to replace, at least in part, the original hand representation affected by the lesion; 4) compared to pre-lesion, there was a post-lesion increase of thresholds at which ICMS elicited movements of the forelimb muscle territories, but again unrelated to the degree of functional recovery; 5) there is preliminary evidence for an enhancement of functional recovery promoted by the anti-Nogo-A antibody treatment, as reflected by the retrieval score for the horizontal slots in the modified Brinkman board task, extending to the non-human primates results previously obtained in rodents (Papadopoulos et al., 2002; Emerick et al., 2003; Emerick and Kartje, 2004; Seymour et al., 2005; Markus et al., 2005; Tsai et al., 2007, 2011; Cheatwood et al., 2008; Gillani et al., 2010).

Although the lesioned hand territory in M1 became, as expected, mostly non-responsive to ICMS, there were some sites where ICMS applied post-lesion elicited movements of the contralateral forelimb (Figs. 1–3). Do they correspond to preserved cortical sites, spared by an insufficient spread of ibotenic acid? This is most likely not the case, as the responsive sites post-lesion do not correspond to zones where the spots selected for infusion of ibotenic acid were more distant from each other than in zones which became completely non-responsive (see e.g. Mk-RO

and Mk-MO). In other words, a deficit of spread of ibotenic acid cannot systematically explain the persistence of micro-excitability sites post-lesion in the cortical area delineated pre-lesion as hand representation. Nevertheless, one cannot totally exclude that few small cortical territories were preserved, as illustrated for Mk-SL in Fig. 4B. Such preserved islands of intact cortex were however rarely observed, as in most monkeys the lesion formed a continuous territory (see Kaeser et al., 2010). Ibotenic acid infusion does not generate a cavity in the cerebral cortex (Peuser et al., 2011), in contrast to a surgical lesion, suggesting that during the period of recovery post-lesion, a few corticospinal neurons or indirect connections to the spinal cord were formed by unknown mechanisms.

In the present study, during the weeks post-lesion there was no sustained rehabilitative training protocol imposed on the monkeys (e.g. constraint induced-therapy), that would complement their daily test sessions. As a consequence, the daily manual dexterity tests correspond to an intermediate motor practice regime. Under these conditions of moderate rehabilitative training, we did not observe any dramatic change of motor maps at the periphery of the lesion in our adult monkeys (e.g. proximal arm/shoulder territory converted into digit sites). Such absence of reappearance of movements previously represented in the lesion zone is reminiscent of the results of Nudo and Milliken (1996), in absence of post-infarct intensive training in adult squirrel monkeys. This situation contrasts with a lesion of M1 performed neonatally in infant monkeys, in which the functional recovery at adult stage was associated with a re-arrangement of the somatotopic representation, with the emergence of a hand territory at a location normally occupied by proximal territories (Rouiller, et al., 1998). There is also a contrast with the data in adult squirrel monkeys obtained by Nudo et al. (1996), who observed a reappearance of hand representations around the lesion in former elbow and shoulder territories, but this change was triggered by a sustained rehabilitative training protocol, not conducted to such an extent in the present study. The present data thus confirm the notion that intensive training is necessary to trigger substantial cortical map reorganization, representing most likely a substrate for an enhanced functional recovery (see Dancause and Nudo for a recent review, 2011). The absence in the present study of cortical map reorganization around the lesion and related to the functional recovery is consistent with previous observations on two control

monkeys subjected to M1 lesion, in which the territory immediately adjacent to the lesion is little, if at all, involved in the recovery, in contrast to the ipsilesional premotor cortex which played a significant role (Liu and Rouiller, 1999). As outlined above, a contribution of the perilesional territory in M1 may appear in the case of a very small lesion of the hand area (Glees and Cole, 1952) or when the lesion is followed by intense rehabilitative therapy (Nudo et al., 1996; Dancause and Nudo, 2011). On the contrary, restricted use of a forelimb leads to a reduction of the corresponding digit representation (Milliken et al., 2013).

An important consideration is the time interval between the cortical lesion and the time point at which the post-lesion ICMS mapping was repeated. In the present study, this time interval was quite variable across monkeys (Table 1) and, in most cases, clearly longer than in the studies conducted on squirrel monkeys by Nudo and collaborators (Nudo and Milliken, 1996; Nudo et al., 1996). Especially in the squirrel monkeys subjected to intensive rehabilitative training (Nudo et al., 1996), the ICMS mapping was repeated early post-lesion (about 5 weeks post-infarct), close to the functional recovery itself (see their Fig. 1). In the present study, as one of our goal was to assess motor performance post-lesion in the long-term (a strategy which has permitted the observation of a second plateau in Mk-VA and Mk-MO in Fig. 8; see also Kaeser et al., 2011 for other monkeys), the time interval was clearly longer. As a consequence, one may not exclude the possibility that motor maps may change when comparing for instance time points such as 1–2 months post-lesion and 5–15 months post-lesion. Indeed, it may be that peri-lesion territories (in the present case wrist, elbow, shoulder), when stimulated, exhibit effects on the digits at low threshold mainly during the restricted time window of the functional recovery itself (before reaching the post-lesion plateau), which are possibly maintained during the first weeks at plateau. Such “early” effects may be explained by rapid unmasking of existent connections to the most distal muscles from proximal territories, mostly silent before the lesion, as proposed by Dancause and Nudo (2011). As the post-lesion mapping conducted in the present study took place later, such early effects may have been less evident.

To explain the absence of re-appearance of hand representation at the immediate periphery of the lesion in the present study (Figs. 1–3), in regions formerly occupied by more proximal territories, it is important

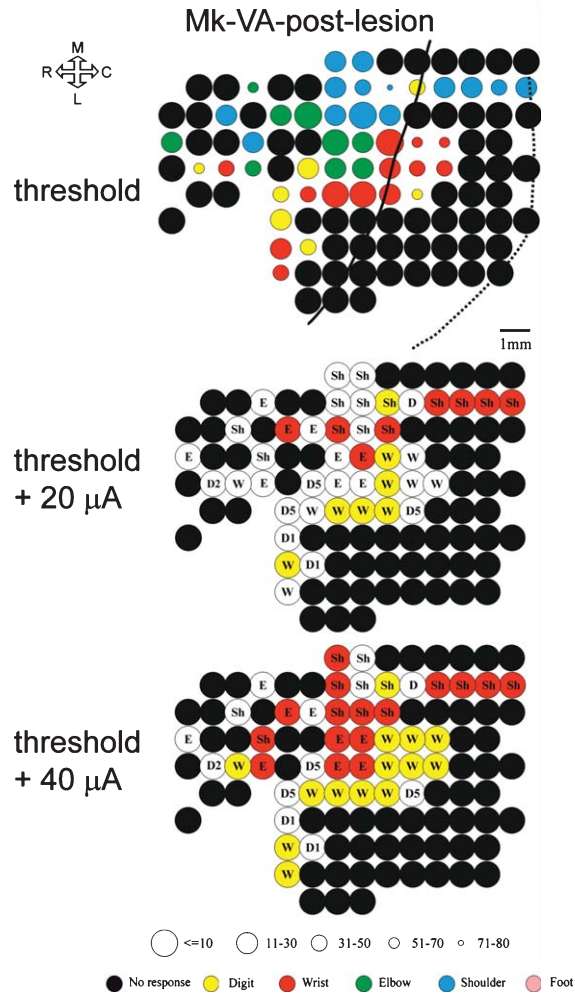


Fig. 11. Modification of unfolded ICMS maps post-lesion for Mk-VA as a function of the current intensity delivered at each stimulation site. The top panel is a repetition of the ICMS map obtained post-lesion at threshold (same as in Fig. 3, top right ICMS map; same conventions as in Fig. 1). In the middle panel, the ICMS map shows some “new” territories activated at 20 microamps above threshold: they are ICMS sites eliciting effect on digit and wrist muscles, depicted in yellow and red, respectively. The muscles activated at threshold at the same sites are indicated in the center of the red or yellow circles by the codes W = wrist, E = elbow and SH = shoulder. The ICMS map in bottom panel shows the effects elicited on digit and wrist muscles at 40 microamps above threshold. In the middle and bottom panels, the white circles are for sites with activation of the same body territories as observed at threshold; the colored circles are for sites at which an additional body territory (more distal) was activated, in addition to the one obtained at threshold (indicated by the letter in the center of the circle). The new territories in red are for additional wrist effects and in yellow are for additional digit effects. Note, as current increased, an increasing recruitment of more distal territories (digits and wrist), in addition to more proximal territories found at threshold for the same site of stimulation.

to remember the strict criterion applied here to establish the ICMS map (Figs. 1–3). The data represent at each stimulation site only the effect elicited by the lowest efficient current (threshold) and not influences on other territories which may occur at somewhat higher currents. In our post-lesion mapping experiments, we indeed also found, at peri-lesion sites representing proximal territories at threshold, ICMS effects on the

digits, but at higher current intensities. In other words, these peri-lesion territories addressing digit motoneurons at higher current intensities (but not visible in the ICMS maps established at threshold) may well be the anatomical support for the restored manual dexterity (wrist and digit movements). The recruitment of additional distal territories post-lesion at current intensities above threshold is illustrated for Mk-VA in Fig. 11. At

both 20 and 40 microamps above threshold, there is evidence of additional effects on digits at sites where more proximal body territories are represented at threshold (wrist, elbow, shoulder), as well as of additional wrist effects at sites representing elbow and shoulder territories at threshold. The same phenomenon as depicted in Fig. 11 for Mk-VA was observed in the other monkeys, irrespective of the anti-Nogo-A antibody treatment. In other words, the anti-Nogo-A antibody treatment did not enhance the appearance of ICMS effects from M1 on digit muscles at current intensities above threshold. Indirectly, this observation suggests that the treatment does not appear to promote restoration of CS projections originating from the lesion territory in M1 or from its immediate surroundings. One may then hypothesize that the anti-Nogo-A antibody treatment may rather enhance compensatory sprouting of efferents or afferents to non-primary motor cortical areas, as observed for the callosal inputs to the ipsilesional PM (Hamadjida et al., 2012).

Based on the retrieval score for the horizontal slots in the modified Brinkman board task, the present study provides further evidence for an enhancement of functional recovery promoted by anti-Nogo-A antibody treatment (Fig. 9, bottom panel). Besides the trend for a better functional recovery in anti-Nogo-A antibody treated monkeys, from the qualitative point of view, two (Mk-MO, Mk-VA) of the three anti-Nogo-A antibody treated monkeys exhibited a rebound in the post-lesion plateau, representing an additional gain of functional recovery whose extent is indicated by the red brackets in Fig. 8B (see also Supplementary video material). The third anti-Nogo-A antibody treated monkey (Mk-SL) did not show such a rebound, but the functional recovery was surprisingly high in spite of a large lesion. The rebound in the post-lesion plateau (Mk-VA and Mk-MO in Fig. 8) is similar to the rebound observed in two monkeys which were transplanted with autologous adult progenitor cells (Kaeser et al., 2011). Interestingly, in sharp contrast, out of five control monkeys subjected to M1 lesion but without any treatment (neither anti-Nogo-A antibody nor progenitor cells transplantation) none exhibited a rebound of functional recovery in the post-lesion plateau (Kaeser et al., 2011). Both treatments (in 4 out of 5 monkeys) thus provide a secondary enhancement of functional recovery, in addition to the level presumably reached by spontaneous recovery. As far as the effect of the anti-Nogo-A antibody treatment is concerned, the present behavioral data based on three treated mon-

keys compared to five control monkeys need to be extended to a larger population of monkeys subjected to a lesion of M1. Nevertheless, the evidence for a beneficial effect of anti-Nogo-A antibody treatment on functional recovery from motor cortex lesion reported here, based on the modified Brinkman board task, is in line with preliminary evidence based on another, complementary manual dexterity test, the Brinkman box (Hamadjida et al., 2012).

From the behavioral point of view, the present study emphasizes the pertinence of horizontal slots in the modified Brinkman board task. It is clearly more challenging than grasping from the vertical slots and it thus represents a more sensitive test, better suited to reflect a benefit of a therapy in our animal model, based on a compromise between a large enough lesion to detect a deficit sufficiently prominent to be compensated better after a treatment and a lesion not too large to avoid a poor condition for the monkeys due to an ethically unacceptable handicap. The sequence of movements to retrieve the pellets from the vertical slots is less difficult than for the pellets in the horizontal slots (see also Freund et al., 2009). For the vertical slots, the monkey performs the precision grip to grasp the pellet, without adjustment of the wrist posture. For the horizontal slots, the monkey has to perform a half pronation or supination of the wrist, followed by the precision grip and a flexion of the wrist. The behavioral data show that the lesioned monkeys have serious difficulty to execute this flexion. Thereby, the initial retrieval score of the two orientations is different and so is the functional recovery after the lesion of M1.

Following lesion of M1 and in the absence of treatment, there is evidence based on reversible inactivation experiments, that "spontaneous" functional recovery depends, at least in part, on the ipsilesional premotor cortex, spared by the injury (Liu and Rouiller, 1999; Hoogewoud et al., 2013). A possible anatomical support for such a vicarious contribution of PM after M1 lesion is the enhancement of the projection of PM to the post-central gyrus (Dancause et al., 2005). Along the same line, there is also anatomical and functional evidence that, after a lesion including M1 and the lateral PM, the ipsilesional SMA contributes to the incomplete functional recovery (McNeal et al., 2010; see also Eisner-Janowicz et al., 2008). In the present study, it is likely that the functional recovery observed in the five control monkeys subjected to M1 lesion results from a substitution to some extent of M1 by non-primary motor cortical areas, especially the ipsilesional PM.

Furthermore, the present ICMS data largely exclude a prominent role played by more proximal territories in M1 spared by the lesion, in line with reversible inactivation experiments conducted in two of the five control monkeys (Liu and Rouiller, 1999). The mechanisms of the vicarious contribution of PM and/or SMA may include sprouting of the corticospinal projections originating from these non-primary areas, as demonstrated for SMA after lesion of M1 and the lateral PM (McNeal et al., 2010). Through its projection to cervical and thoracic segments of the spinal cord (Rouiller et al., 1996; Dum and Strick, 1991), SMA is in position to take over some direct influence of M1 on hand motoneurons, though to a limited extent as its influence on distal motoneurons in the normal function is clearly less prominent than corticospinal inputs arising from M1 (Maier et al., 2002; Boudrias et al., 2006, 2010a). For PM, its corticospinal projection exerts effects on distal motoneurons, but they are also clearly lower than those originating from M1 (Boudrias et al., 2010b), reflecting mainly an indirect linkage with the motoneurons. In particular, PMv was shown to exert an influence mostly via its cortico-cortical projection to M1 (Cerri et al., 2003; Shimazu et al., 2004; Schmidlin et al., 2008; Prabhu et al., 2009), although some descending influence via intraspinal circuits in the spinal cord cannot be excluded (Sasaki et al., 2004; Takei and Seki, 2010; Alstermark et al., 2011; Kinoshita et al., 2012). Contributions of non-primary motor cortical areas to the functional recovery after lesion of M1, irrespective of whether they are direct or indirect, can be interpreted as an unmasking of pre-existing, but mostly silent, projections and/or axonal sprouting forming new connections (see Dancause and Nudo, 2011 for a recent review). It is likely that the anti-Nogo-A antibody treatment may have enhanced some axonal sprouting, especially involving the ipsilesional PM, as observed for the callosal projections from the intact hemisphere terminating in the ipsilesional PM (Hamadjida et al., 2012). Whether other connections of PM (or of other cortical areas, for instance SMA), such as their corticospinal, corticorubral and corticobulbar projections have also been promoted by the anti-Nogo-A antibody treatment remains an open question at present. As the anti-Nogo-A antibody was delivered not only around the lesion at cortical level, but also at cervical level, an enhancement of re-organization of intraspinal circuits may also have promoted functional recovery (Bareyre et al., 2004).

The current pre-lesion ICMS maps shown in Figs. 1–3 for *macaca fascicularis* are fully consistent

with previously published representations of the output map of M1 in macaque monkeys (*macaca mulata*), using the same unfolding procedure of the rostral bank of the central sulcus (Park et al., 2001, 2004): the extent of the distal (digits) representation is highly comparable, as well as the surrounding of the digits' area by more proximal territories (wrist, elbow, shoulder) medially, rostrally and also laterally, but to a much smaller extent (e.g. Mk-BI and Mk-JU for instance). However, laterally to the digits' area, most ICMS sites elicit movements of face muscles (Park et al., 2001, 2004; present study: not shown). Moreover, the pre-lesion ICMS maps in Figs. 1–3 confirm the presence of some overlap of the external rim of the digits' area with more proximal territories, as reported by Park et al. (2001, 2004). The pre-lesion raw ICMS maps established in the present study (as shown in Fig. 1 for Mk-BI) are also consistent with previously published ICMS data for intact macaque monkeys, but without unfolding procedure (e.g. Kwan et al., 1978; Sessle and Wiesendanger, 1982; Humphrey, 1986; Lemon, 1988; Aizawa et al., 1990).

In conclusion, the present study shows that the re-arrangement of motor maps in and around the lesioned territory in M1 is variable across monkeys, but without obvious relationship to the degree of functional recovery of manual dexterity. This conclusion holds for experimental conditions in which there was no intensive rehabilitative training during the weeks post-lesion. The situation is likely to be different in cases of more intensive rehabilitative training (see Nudo and Milliken, 1996; Nudo et al., 1996; Friel et al., 2000). Nevertheless, in the absence of such training, there is evidence that some functional restitution of manual dexterity after lesion of the hand representation in M1 in the adult macaque depends to a large extent on the vicarious role played by non primary motor areas (PM, SMA: see Liu and Rouiller, 1999; Eisner-Janowicz et al., 2008; Mc Neal et al., 2010). A significant rehabilitative therapy protocol needs to be implemented in order to favor the re-arrangement of the motor map in the immediate vicinity of the lesion (and perhaps also enhance the contribution of non-primary motor areas), although care should be taken to adopt the most adequate timing of such interventions. In addition, therapies such as neutralization of nerve growth inhibitors (present study; Hamadjida et al., 2012) or cell therapy (Kaeser et al., 2011) may further boost the capacity of functional restitution, although a larger number of monkeys is needed

to better decipher the precise mechanisms of such enhancements.

## Acknowledgments

The authors wish to thank the technical assistance of Véronique Moret, Christine Roulin, Françoise Tinguely, Christiane Marti (histology), Alexandra Meszaros (lesion reconstruction), Eric Schmidlin, Jocelyne Bloch, Jean-François Brunet, Mélanie Kaeser (for contributing to some experiments), Josef Corpataux, Laurent Bossy (animal care taking), André Gaillard (mechanics), Bernard Aebischer (electronics), Laurent Monney (informatics). We thank Dr. Jennifer Miles-Chan for editing the manuscript.

Grant sponsors: Swiss National Science Foundation, Grants No. 31-61857.00, 310000-110005, 31003A-132465 (EMR), and 3100-063633, 31003A122527 (MES), the National Centre of Competence in Research (NCCR) on “Neural plasticity and repair”; Novartis Foundation; The Christopher Reeves Foundation (Springfield, NJ, USA); The Swiss Primate Competence Centre for Research (SPCCR: <http://www.unifr.ch/neuro/rouiller/SPCCR/welcome.html>).

## Conflict of interest

The anti-Nogo-A antibody was provided by Novartis Pharma AG.

## Supplementary video material

Manual dexterity performance is illustrated in the form of video sequences at different time points (pre-lesion, post-lesion immediately after the lesion, at post-lesion plateau) for the control Mk-BI and the anti-Nogo-A antibody treated Mk-VA (see text in the results section). The video sequences are accessible at: <http://www.unifr.ch/neuro/rouiller/FRJS/index.html>

## References

- [1] Aizawa, H., Mushiaki, H., Inase, M., & Tanji, J. (1990). An output zone of the monkey primary motor cortex specialized for bilateral hand movement. *Exp Brain Res*, *82*, 219-221.
- [2] Alstermark, B., Pettersson, L.G., Nishimura, Y., Yoshino-Saito, K., Tsuboi, F., Takahashi, M., & Isa, T. (2011). Motor command for precision grip in the macaque monkey can be mediated by spinal interneurons. *J Neurophysiol*, *106*, 122-126.
- [3] Bareyre, F.M., Kerschensteiner, M., Raineteau, O., Mettenleiter, T.C., Weinmann, O., & Schwab, M.E. (2004). The injured spinal cord spontaneously forms a new intraspinal circuit in adult rats. *Nat Neurosci*, *7*, 269-277.
- [4] Bashir, S., Kaeser, M., Wyss, A., Hamadjida, A., Liu, Y., Bloch, J., Brunet, J.F., Belhaj-Saif, A., & Rouiller, E.M. (2012). Short-term effects of unilateral lesion of the primary motor cortex (M1) on ipsilesional hand dexterity in adult macaque monkeys. *Brain Struct Funct*, *217*, 63-79.
- [5] Beaud, M.L., Schmidlin, E., Wannier, T., Freund, P., Bloch, J., Mir, A., Schwab, M.E., & Rouiller, E.M. (2008). Anti-Nogo-A antibody treatment does not prevent cell body shrinkage in the motor cortex in adult monkeys subjected to unilateral cervical cord lesion. *BMC Neurosci*, *9*, 5.
- [6] Bihel, E., Pro-Sistiaga, P., Letourneur, A., Toutain, J., Saulnier, R., Insausti, R., Bernaudin, M., Roussel, S., & Touzani, O. (2010). Permanent or transient chronic ischemic stroke in the non-human primate: Behavioral, neuroimaging, histological, and immunohistochemical investigations. *J Cereb Blood Flow Metab*, *30*, 273-285.
- [7] Boudrias, M.H., Belhaj-Saif, A., Park, M.C., & Cheney, P.D. (2006). Contrasting properties of motor output from the supplementary motor area and primary motor cortex in rhesus macaques. *Cereb Cortex*, *16*, 632-638.
- [8] Boudrias, M.H., Lee, S.P., Svojanovsky, S., & Cheney, P.D. (2010a). Forelimb muscle representations and output properties of motor areas in the mesial wall of rhesus macaques. *Cereb Cortex*, *20*, 704-719.
- [9] Boudrias, M.H., McPherson, R.L., Frost, S.B., & Cheney, P.D. (2010b). Output properties and organization of the forelimb representation of motor areas on the lateral aspect of the hemisphere in rhesus macaques. *Cereb Cortex*, *20*, 169-186.
- [10] Brinkman, C. (1984). Supplementary motor area of the monkey's cerebral cortex: Short- and long-term deficits after unilateral ablation and the effects of subsequent callosal section. *J Neurosci*, *4*, 918-929.
- [11] Brinkman, J., & Kuypers, H.G.J.M. (1973). Cerebral control of contralateral and ipsilateral arm, hand and finger movements in the split-brain rhesus monkey. *Brain*, *96*, 653-674.
- [12] Cerri, G., Shimazu, H., Maier, M.A., & Lemon, R.N. (2003). Facilitation from ventral premotor cortex of primary motor cortex outputs to macaque hand muscles. *J Neurophysiol*, *90*, 832-842.
- [13] Cheatwood, J.L., Emerick, A.J., Schwab, M.E., & Kartje, G.L. (2008). Nogo-A expression after focal ischemic stroke in the adult rat. *Stroke*, *39*, 2091-2098.
- [14] Courtine, G., Bunge, M.B., Fawcett, J.W., Grossman, R.G., Kaas, J.H., Lemon, R., Maier, I., Martin, J., Nudo, R.J., Ramon-Cueto, A., Rouiller, E.M., Schnell, L., Wannier, T., Schwab, M.E., & Edgerton, V.R. (2007). Can experiments in nonhuman primates expedite the translation of treatments for spinal cord injury in humans? *Nat Med*, *13*, 561-566.
- [15] Dancause, N., Barbay, S., Frost, S.B., Plautz, E.J., Chen, D.F., Zoubina, E.V., Stowe, A.M., & Nudo, R.J. (2005). Extensive cortical rewiring after brain injury. *J Neurosci*, *25*, 10167-10179.
- [16] Dancause, N., Barbay, S., Frost, S.B., Zoubina, E.V., Plautz, E.J., Mahnken, J.D., & Nudo, R.J. (2006). Effects of small ischemic lesions in the primary motor cortex on neu-

- rophysiological organization in ventral premotor cortex. *J Neurophysiol*, 96, 3506-3511.
- [17] Dancause, N., & Nudo, R.J. (2011). Shaping plasticity to enhance recovery after injury. *Prog Brain Res*, 192, 273-295.
- [18] Darling, W.G., Pizzimenti, M.A., Rotella, D.L., Peterson, C.R., Hynes, S.M., Ge, J., Solon, K., McNeal, D.W., Stilwell-Morecraft, K.S., & Morecraft, R.J. (2009). Volumetric effects of motor cortex injury on recovery of dexterous movements. *Exp Neurol*, 220, 90-108.
- [19] Darling, W.G., Pizzimenti, M.A., Rotella, D.L., Hynes, S.M., Ge, J., Stilwell-Morecraft, K.S., Vanadurongvan, T., McNeal, D.W., Solon-Cline, K.M., & Morecraft, R.J. (2010). Minimal forced use without constraint stimulates spontaneous use of the impaired upper extremity following motor cortex injury. *Exp Brain Res*, 202, 529-542.
- [20] Darling, W.G., Pizzimenti, M.A., Hynes, S.M., Rotella, D.L., Headley, G., Ge, J., Stilwell-Morecraft, K.S., McNeal, D.W., Solon-Cline, K.M., & Morecraft, R.J. (2011). Volumetric effects of motor cortex injury on recovery of ipsilesional dexterous movements. *Exp Neurol*, 231, 56-71.
- [21] Dum, R.P., & Strick, P.L. (1991). The origin of corticospinal projections from the premotor areas in the frontal lobe. *J Neurosci*, 11, 667-689.
- [22] Eisner-Janowicz, I., Barbay, S., Hoover, E., Stowe, A.M., Frost, S.B., Plautz, E.J., & Nudo, R.J. (2008). Early and late changes in the distal forelimb representation of the supplementary motor area after injury to frontal motor areas in the squirrel monkey. *J Neurophysiol*, 100, 1498-1512.
- [23] Emerick, A.J., Neafsey, E.J., Schwab, M.E., & Kartje, G.L. (2003). Functional reorganization of the motor cortex in adult rats after cortical lesion and treatment with monoclonal antibody IN-1. *J Neurosci*, 23, 4826-4830.
- [24] Emerick, A.J., & Kartje, G.L. (2004). Behavioral recovery and anatomical plasticity in adult rats after cortical lesion and treatment with monoclonal antibody IN-1. *Behav. Brain Res*, 152, 315-325.
- [25] Freund, P., Schmidlin, E., Wannier, T., Bloch, J., Mir, A., Schwab, M.E., & Rouiller, E.M. (2006). Nogo-A-specific antibody treatment enhances sprouting and functional recovery after cervical lesion in adult primates. *Nature Med*, 12, 790-792.
- [26] Freund, P., Wannier, T., Schmidlin, E., Bloch, J., Mir, A., Schwab, M.E., & Rouiller, E.M. (2007). Anti-Nogo-A antibody treatment enhances sprouting of corticospinal axons rostral to a unilateral cervical spinal cord lesion in adult macaque monkey. *J Comp Neurol*, 502, 644-659.
- [27] Freund, P., Schmidlin, E., Wannier, T., Bloch, J., Mir, A., Schwab, M.E., & Rouiller, E.M. (2009). Anti-Nogo-A antibody treatment promotes recovery of manual dexterity after unilateral cervical lesion in adult primates—re-examination and extension of behavioral data. *Eur J Neurosci*, 29, 983-996.
- [28] Friel, K.M., & Nudo, R.J. (1998). Recovery of motor function after focal cortical injury in primates: Compensatory movement patterns used during rehabilitative training. *Somatosens Mot Res*, 15, 173-189.
- [29] Friel, K.M., Heddings, A.A., & Nudo, R.J. (2000). Effects of postlesion experience on behavioral recovery and neurophysiologic reorganization after cortical injury in primates. *Neurorehabil Neural Repair*, 14, 187-198.
- [30] Frost, S.B., Barbay, S., Friel, K.M., Plautz, E.J., & Nudo, R.J. (2003). Reorganization of remote cortical regions after ischemic brain injury: A potential substrate for stroke recovery. *J Neurophysiol*, 89, 3205-3214.
- [31] Gillani, R.L., Tsai, S.Y., Wallace, D.G., O'Brien, T.E., Arhebamen, E., Tole, M., Schwab, M.E., & Kartje, G.L. (2010). Cognitive recovery in the aged rat after stroke and anti-Nogo-A immunotherapy. *Behav Brain Res*, 208, 415-424.
- [32] Glees, P., & Cole, J. (1950). Recovery of skilled motor function after small repeated lesions of motor cortex in macaque. *J Neurophysiol*, 13, 137-148.
- [33] Gonzenbach, R.R., & Schwab, M.E. (2008). Disinhibition of neurite growth to repair the injured adult CNS: Focusing on Nogo. *Cell Mol Life Sci*, 65, 161-176.
- [34] Hamadjida, A., Wyss, A.F., Mir, A., Schwab, M.E., Belhaj-Saif, A., & Rouiller, E.M. (2012). Influence of anti-Nogo-A antibody treatment on the reorganization of callosal connectivity of the premotor cortical areas following unilateral lesion of primary motor cortex (M1) in adult macaque monkeys. *Exp Brain Res*, 223, 321-340.
- [35] He, S.Q., Dum, R.P., & Strick, P.L. (1993). Topographic organization of corticospinal projections from the frontal lobe: Motor areas on the lateral surface of the hemisphere. *J Neurosci*, 13, 952-980.
- [36] He, S.Q., Dum, R.P., & Strick, P.L. (1995). Topographic organization of corticospinal projections from the frontal lobe: Motor areas on the medial surface of the hemisphere. *J Neurosci*, 15, 3284-3306.
- [37] Hoogewoud, F., Hamadjida, A., Wyss, A.F., Mir, A., Schwab, M.E., Belhaj-Saif, A., & Rouiller, E.M. (2013). Comparison of functional recovery of manual dexterity after unilateral spinal cord lesion or motor cortex lesion in adult macaque monkeys. *Front Neurol*, 4, 101.
- [38] Humphrey, D.R. (1986). Representation of movements and muscles within the primate precentral. *Fed Proc*, 45, 2687-2699.
- [39] Kaeser, M., Wyss, A.F., Bashir, S., Hamadjida, A., Liu, Y., Bloch, J., Brunet, J.F., Belhaj-Saif, A., & Rouiller, E.M. (2010). Effects of Unilateral Motor Cortex Lesion on Ipsilesional Hand's Reach and Grasp Performance in Monkeys: Relationship With Recovery in the Contralateral Hand. *J Neurophysiol*, 103, 1630-1645.
- [40] Kaeser, M., Brunet, J.F., Wyss, A., Belhaj-Saif, A., Liu, Y., Hamadjida, A., Rouiller, E.M., & Bloch, J. (2011). Autologous adult cortical cell transplantation enhances functional recovery following unilateral lesion of motor cortex in primates: A pilot study. *Neurosurgery*, 68, 1405-1417.
- [41] Kaeser, M., Wannier, T., Brunet, J.F., Wyss, A., Bloch, J., & Rouiller, E.M. (2013). Representation of motor habit in a sequence of repetitive reach and grasp movements performed by macaque monkeys: Evidence for a contribution of the dorsolateral prefrontal cortex. *Cortex*, 49, 1404-1419.
- [42] Kinoshita, M., Matsui, R., Kato, S., Hasegawa, T., Kasahara, H., Isa, K., Watakabe, A., Yamamori, T., Nishimura, Y., Alstermark, B., Watanabe, D., Kobayashi, K., & Isa, T. (2012). Genetic dissection of the circuit for hand dexterity in primates. *Nature*, 487, 235-238.
- [43] Kwan, H.C., MacKay, W.A., Murphy, J.T., & Wong, Y.C. (1978). Spatial organization of precentral cortex in awake primates. II. Motor outputs. *J Neurophysiol*, 41, 1120-1131.
- [44] Lemon, R. (1988). The output map of the primate motor cortex. *Trends Neurosci*, 11, 501-506.
- [45] Lemon, R.N., & Griffiths, J. (2005). Comparing the function of the corticospinal system in different species: Organiza-

- tional differences for motor specialization? *Muscle Nerve*, *32*, 261-279.
- [46] Lemon, R.N. (2008). Descending pathways in motor control. *Annu Rev Neurosci*, *31*, 195-218.
- [47] Liu, J., Morel, A., Wannier, T., & Rouiller, E.M. (2002). Origins of callosal projections to the supplementary motor area (SMA): A direct comparison between pre-SMA and SMA-proper in macaque monkeys. *J Comp Neurol*, *443*, 71-85.
- [48] Liu, Y., & Rouiller, E.M. (1999). Mechanisms of recovery of dexterity following unilateral lesion of the sensorimotor cortex in adult monkeys. *Exp Brain Res*, *128*, 149-159.
- [49] Maier, M.A., Armand, J., Kirkwood, P.A., Yang, H.W., Davis, J.N., & Lemon, R.N. (2002). Differences in the corticospinal projection from primary motor cortex and supplementary motor area to macaque upper limb motoneurons: An anatomical and electrophysiological study. *Cereb. Cortex*, *12*, 281-296.
- [50] Markus, T.M., Tsai, S.Y., Bollnow, M.R., Farrer, R.G., O'Brien, T.E., Kindler-Baumann, D.R., Rausch, M., Rudin, M., Wiessner, C., Mir, A.K., Schwab, M.E., & Kartje, G.L. (2005). Recovery and brain reorganization after stroke in adult and aged rats. *Ann Neurol*, *58*, 950-953.
- [51] Marshall, J.W., Ridley, R.M., Baker, H.F., Hall, L.D., Carpenter, T.A., & Wood, N.I. (2003). Serial MRI, functional recovery, and long-term infarct maturation in a non-human primate model of stroke. *Brain Res Bull*, *61*, 577-585.
- [52] Martin, J.H. (1991). Autoradiographic estimation of the extent of reversible inactivation produced by microinjection of lidocaine and muscimol in the rat. *Neurosci Lett*, *127*, 160-164.
- [53] McNeal, D.W., Darling, W.G., Ge, J., Stilwell-Morecraft, K.S., Solon, K.M., Hynes, S.M., Pizzimenti, M.A., Rotella, D.L., Vanadurongvan, T., & Morecraft, R.J. (2010). Selective long-term reorganization of the corticospinal projection from the supplementary motor cortex following recovery from lateral motor cortex injury. *J Comp Neurol*, *518*, 586-621.
- [54] Milliken, G.W., Plautz, E.J., & Nudo, R.J. (2013). Distal forelimb representations in primary motor cortex are redistributed after forelimb restriction: A longitudinal study in adult squirrel monkeys. *J Neurophysiol*, *109*, 1268-1282.
- [55] Murata, Y., Higo, N., Oishi, T., Yamashita, A., Matsuda, K., Hayashi, M., & Yamane, S. (2008). Effects of motor training on the recovery of manual dexterity after primary motor cortex lesion in macaque monkeys. *J Neurophysiol*, *99*, 773-786.
- [56] Nudo, R.J., Wise, B.M., SiFuentes, F., & Milliken, G.W. (1996). Neural substrates for the effects of rehabilitative training on motor recovery after ischemic infarct. *Science*, *272*, 1791-1794.
- [57] Nudo, R.J., & Milliken, G.W. (1996). Reorganization of movement representations in primary motor cortex following focal ischemic infarcts in adult squirrel monkeys. *J Neurophysiol*, *75*, 2144-2149.
- [58] Oertle, T., Van der Haar, M.E., Bandtlow, C.E., Robeva, A., Burfeind, P., Buss, A., Huber, A.B., Simonen, M., Schnell, L., Brösamle, C., Kaupmann, K., Vallon, R., & Schwab, M.E. (2003). Nogo-A inhibits neurite outgrowth and cell spreading with three discrete regions. *J Neurosci*, *23*, 5393-5406.
- [59] Ogden, R., & Franz, S.I. (1917). On cerebral motor control: The recovery from experimentally produced hemiplegia. *Psychobiology*, *1*, 33-49.
- [60] Papadopoulos, C.M., Tsai, S.Y., Alsbjæ, T., O'Brien, T.E., Schwab, M.E., & Kartje, G.L. (2002). Functional recovery and neuroanatomical plasticity following middle cerebral artery occlusion and IN-1 antibody treatment in the adult rat. *Ann Neurol*, *51*, 433-441.
- [61] Park, M.C., Belhaj-Saif, A., Gordon, M., & Cheney, P.D. (2001). Consistent features in the forelimb representation of primary motor cortex in rhesus macaques. *J Neurosci*, *21*, 2784-2792.
- [62] Park, M.C., Belhaj-Saif, A., & Cheney, P.D. (2004). Properties of primary motor cortex output to forelimb muscles in rhesus macaques. *J Neurophysiol*, *92*, 2968-2984.
- [63] Passingham, R.E., Perry, V.H., & Wilkinson, F. (1983). The long-term effects of removal of sensorimotor cortex in infant and adult rhesus monkeys. *Brain*, *106*(Pt 3), 675-705.
- [64] Peuser, J., Belhaj-Saif, A., Hamadjida, A., Schmidlin, E., Gindrat, A.D., Volker, A.C., Zakharov, P., Hoogewoud, H.M., Rouiller, E.M., & Scheffold, F. (2011). Follow-up of cortical activity and structure after lesion with laser speckle imaging and magnetic resonance imaging in nonhuman primates. *J Biomed Opt*, *16*, 096011.
- [65] Pizzimenti, M.A., Darling, W.G., Rotella, D.L., McNeal, D.W., Herrick, J.L., Ge, J., Stilwell-Morecraft, K.S., & Morecraft, R.J. (2007). Measurement of reaching kinematics and prehensile dexterity in nonhuman primates. *J Neurophysiol*, *98*, 1015-1029.
- [66] Plautz, E.J., Barbay, S., Frost, S.B., Friel, K.M., Dancause, N., Zoubina, E.V., Stowe, A.M., Quaney, B.M., & Nudo, R.J. (2003). Post-infarct cortical plasticity and behavioral recovery using concurrent cortical stimulation and rehabilitative training: A feasibility study in primates. *Neurol Res*, *25*, 801-810.
- [67] Prabhu, G., Shimazu, H., Cerri, G., Brochier, T., Spinks, R.L., Maier, M.A., & Lemon, R.N. (2009). Modulation of primary motor cortex outputs from ventral premotor cortex during visually guided grasp in the macaque monkey. *J Physiol*, *587*, 1057-1069.
- [68] Rathelot, J.A., & Strick, P.L. (2006). Muscle representation in the macaque motor cortex: An anatomical perspective. *Proc Natl Acad Sci U. S. A*, *103*, 8257-8262.
- [69] Ruitberg, B., Khan, N., Tuccar, E., Kompoliti, K., Chu, Y., Alperin, N., Kordower, J.H., & Emborg, M.E. (2003). Chronic ischemic stroke model in cynomolgus monkeys: Behavioral, neuroimaging and anatomical study. *Neurol Res*, *25*, 68-78.
- [70] Rouiller, E.M., Moret, V., Tanné, J., & Boussaoud, D. (1996). Evidence for direct connections between the hand region of the supplementary motor area and cervical motoneurons in the macaque monkey. *Eur J Neurosci*, *8*, 1055-1059.
- [71] Rouiller, E.M., Yu, X.H., Moret, V., Tempini, A., Wiesendanger, M., & Liang, F. (1998). Dexterity in adult monkeys following early lesion of the motor cortical hand area: The role of cortex adjacent to the lesion. *Eur J Neurosci*, *10*, 729-740.
- [72] Sasaki, K., & Gemba, H. (1984). Compensatory motor function of the somatosensory cortex for dysfunction of the motor cortex following cerebellar hemispherectomy in the monkey. *Exp Brain Res*, *56*, 532-538.
- [73] Sasaki, S., Isa, T., Pettersson, L.G., Alstermark, B., Naito, K., Yoshimura, K., Seki, K., & Ohki, Y. (2004). Dexterous finger movements in primate without monosynaptic corticomotoneuronal excitation. *J Neurophysiol*, *92*, 3142-3147.
- [74] Schmidlin, E., Wannier, T., Bloch, J., & Rouiller, E.M. (2004). Progressive plastic changes in the hand representation of the primary motor cortex parallel incomplete recovery from a unilateral section of the corticospinal tract at cervical level in monkeys. *Brain Research*, *1017*, 172-183.

- [75] Schmidlin, E., Wannier, T., Bloch, J., Belhaj-Saif, A., Wyss, A., & Rouiller, E.M. (2005). Reduction of the hand representation in the ipsilateral primary motor cortex following unilateral section of the corticospinal tract at cervical level in monkeys. *BMC Neuroscience*, 6, 56.
- [76] Schmidlin, E., Brochier, T., Maier, M.A., Kirkwood, P.A., & Lemon, R.N. (2008). Pronounced reduction of digit motor responses evoked from macaque ventral premotor cortex after reversible inactivation of the primary motor cortex hand area. *J Neurosci*, 28, 5772-5783.
- [77] Schmidlin, E., Kaeser, M., Gindrat, A.D., Savidan, J., Chatagny, P., Badoud, S., Hamadjida, A., Beaud, M.L., Wannier, T., Belhaj-Saif, A., & Rouiller, E.M. (2011). Behavioral assessment of manual dexterity in non-human primates. *J Vis Exp*, 3258.
- [78] Schwab, M.E. (2010). Functions of Nogo proteins and their receptors in the nervous system. *Nat Rev Neurosci*, 11, 799-811.
- [79] Sessle, B.J., & Wiesendanger, M. (1982). Structural and functional definition of the motor cortex in the monkey (macaca fascicularis). *J Physiol (London)*, 323, 245-265.
- [80] Seymour, A.B., Andrews, E.M., Tsai, S.Y., Markus, T.M., Bollnow, M.R., Brenneman, M.M., O'Brien, T.E., Castro, A.J., Schwab, M.E., & Kartje, G.L. (2005). Delayed treatment with monoclonal antibody IN-1 1 week after stroke results in recovery of function and corticorubral plasticity in adult rats. *J Cereb. Blood Flow Metab*, 25, 1366-1375.
- [81] Shimazu, H., Maier, M.A., Cerri, G., Kirkwood, P.A., & Lemon, R.N. (2004). Macaque ventral premotor cortex exerts powerful facilitation of motor cortex outputs to upper limb motoneurons. *J Neurosci*, 24, 1200-1211.
- [82] Snyder, G.L., Galdi, S., Hendrick, J.P., & Hemmings, H.C. Jr (2007). General anesthetics selectively modulate glutamatergic and dopaminergic signaling via site-specific phosphorylation *in vivo*. *Neuropharmacology*, 53, 619-630.
- [83] Takei, T., & Seki, K. (2010). Spinal interneurons facilitate coactivation of hand muscles during a precision grip task in monkeys. *J Neurosci*, 30, 17041-17050.
- [84] Travis, A.M. (1955). Neurological deficiencies after ablation of the precentral motor area in Macaca mulatta. *Brain*, 78, 155-173.
- [85] Tsai, S.Y., Markus, T.M., Andrews, E.M., Cheatwood, J.L., Emerick, A.J., Mir, A.K., Schwab, M.E., & Kartje, G.L. (2007). Intrathecal treatment with anti-Nogo-A antibody improves functional recovery in adult rats after stroke. *Exp Brain Res*, 182, 261-266.
- [86] Tsai, S.Y., Papadopoulos, C.M., Schwab, M.E., & Kartje, G.L. (2011). Delayed anti-nogo-a therapy improves function after chronic stroke in adult rats. *Stroke*, 42, 186-190.
- [87] Wannier, T., Schmidlin, E., Bloch, J., & Rouiller, E.M. (2005). A unilateral section of the corticospinal tract at cervical level in primate does not lead to measurable cell loss in motor cortex. *J Neurotrauma*, 22, 703-717.
- [88] Widener, G.L., & Cheney, P.D. (1997). Effects on muscle activity from microstimuli applied to somatosensory and motor cortex during voluntary movement in the monkey. *J Neurophysiol*, 77, 2446-2465.